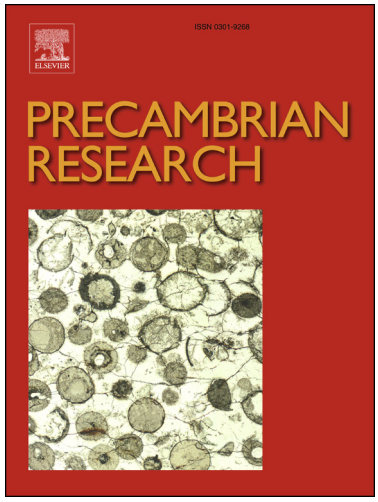

The origin of the Palaeoproterozoic AMCG complexes in the Ukrainian Shield: new U-Pb ages and Hf isotopes in zircon

Leonid Shumlyanskyy, Chris Hawkesworth, Kjell Billström, Svetlana Bogdanova, Oleksandr Mytrokhyn, Rolf Romer, Bruno Dhuime, Stefan Claesson, Richard Ernst, Martin Whitehouse, Olena Bilan

PII: S0301-9268(16)30239-X
DOI: http://dx.doi.org/10.1016/j.precamres.2017.02.009
Reference: PRECAM 4674

To appear in: *Precambrian Research*

Received Date: 1 July 2016
Revised Date: 21 December 2016
Accepted Date: 15 February 2017

Please cite this article as: L. Shumlyanskyy, C. Hawkesworth, K. Billström, S. Bogdanova, O. Mytrokhyn, R. Romer, B. Dhuime, S. Claesson, R. Ernst, M. Whitehouse, O. Bilan, The origin of the Palaeoproterozoic AMCG complexes in the Ukrainian Shield: new U-Pb ages and Hf isotopes in zircon, *Precambrian Research* (2017), doi: http://dx.doi.org/10.1016/j.precamres.2017.02.009

The origin of the Palaeoproterozoic AMCG complexes in the Ukrainian Shield: new U-Pb ages and Hf isotopes in zircon

Leonid Shumlyanskyy[a], Chris Hawkesworth[b,c], Kjell Billström[d], Svetlana Bogdanova[e], Oleksandr Mytrokhyn[f], Rolf Romer[g], Bruno Dhuime[c], Stefan Claesson[d], Richard Ernst[h, i], Martin Whitehouse[d], Olena Bilan[f]

[a]M.P. Semenenko Institute of Geochemistry, Mineralogy and Ore Formation, Palladina ave., 34, 03680, Kyiv, Ukraine. E-mail: lshumlyanskyy@yahoo.com

[b]Earth and Environmental Sciences, University of St. Andrews, College Gate, North Street, St. Andrews, KY16 9AJ, UK

[c] Department of Earth Sciences, University of Bristol, Queen's Road, Bristol, BS8 1RJ, UK

[d]Department of Geological Sciences, Swedish Museum of Natural History, Box 50007, SE-10405 Stockholm, Sweden

[e] Department of Geology, Lund University, Sölvegatan 12, SE 223 62 Lund, Sweden

[f] Department of Geology, Kyiv Taras Shevchenko National University, Vasylkivska st., 90, 03022, Kyiv, Ukraine

[g] GFZ German Research Centre for Geosciences, Telegrafenberg, Building B, 14473 Potsdam, Germany

[h]Department of Earth Sciences, Carleton University, Ottawa, Ontario, Canada

[i]Faculty of Geology and Geography, Tomsk State University, 36 Lenin Ave, Tomsk 634050, Russia

The Ukrainian shield hosts two Palaeoproterozoic anorthosite-mangerite-charnockite-granite (AMCG) complexes (the Korosten and Korsun-Novomyrhorod complexes) that intruded Palaeoproterozoic continental crust in north-western and central parts of the shield,

respectively. We report results of U-Pb zircon and baddeleyite dating of 16 samples from the Korosten plutonic complex (KPC), and 6 samples from the Korsun-Novomyrhorod plutonic complex (KNPC). Fifteen zircon samples from both complexes were also analysed for Hf isotopes. These new, together with previously published data indicate that the formation of the KPC started at c. 1815 Ma and continued until 1743 Ma with two main phases of magma emplacement at 1800-1780 and 1770-1758 Ma. Each of the main phases of magmatic activity included both basic and silicic members. The emplacement history of the KNPC is different from that of the KPC. The vast majority of the KNPC basic and silicic rocks were emplaced between c. 1757 and 1750 Ma; the youngest stages of the complex are represented by monzonites and syenites that were formed between 1748 and 1744 Ma. Both Ukrainian AMCG complexes are closely associated in space and time with mantle-derived mafic and ultramafic dykes. The Hf isotope ratios in the zircons indicate a predominantly crustal source for the initial melts with some input of juvenile Hf from mantle-derived tholeiite melts.

The preferred model for the formation of the Ukrainian AMCG complexes involves the emplacement of large volumes of hot mantle-derived tholeiitic magma into the lower crust. This resulted in partial melting of mafic lower-crustal material, mixing of lower crustal and tholeiitic melts, and formation of ferromonzodioritic magmas. Further fractional crystallization of the ferromonzodioritic melts produced the spectrum of basic rocks in the AMCG complexes. Emplacement of the ferromonzodioritic and tholeiitic melts into the middle crust and their partial crystallization caused abundant melting of the ambient crust and formation of the large volumes of granitic rocks present in the complexes.

KEY WORDS: *AMCG complexes; Hf isotopes; Proterozoic; Ukrainian shield; U-Pb geochronology.*

1. Introduction

The origin of anorthosite-mangerite-charnockite-granite (AMCG) complexes is one of the more intriguing problems of modern petrology. The main aspects include the origin and nature of the initial melts, and the relationships between silicic and basic members of the AMCG associations. Different researchers have proposed models in which the initial source was in the mantle (Ashwal et al., 1986; Ashwal, 1993; Emslie and Hegner, 1993; Scoates and Frost, 1996; Frost and Frost, 1997; Gleißner et al., 2011) or in the lower crust (Taylor et al., 1984; Schärer et al., 1996; Longhi et al., 1999; Duchesne et al., 1999; Schiellerup et al., 2000; Longhi, 2005). In some cases more complex models of interaction of initial mantle melts with reworked crustal material were preferred (Emslie et al., 1994; Rämö and Haapala, 2005). As for the AMCG complexes, a number of relationships between the basic and silicic members have been proposed. The first model envisages common parental melts that underwent fractional crystallization to produce the spectrum of rocks from basic to granitic (e.g. Duchesne and Wilmart, 1997; Vander Auwera et al., 1998). The second type of model invokes indirect links between silicic and basic melts that originate due to common processes but from different sources (Emslie, 1991; Rämö and Haapala, 1996; Bolle et al., 2003; Wilson and Overgaard, 2005; Duchesne et al., 2010).

AMCG complexes worldwide exhibit some similarities with respect to their emplacement history. They commonly developed over prolonged periods of time that may extend for up to several tens of millions of years (M.y.) (Vaasjoki et al., 1991; Higgins and van Breemen, 1996; Amelin et al., 1997, 1999; Alviola et al., 1999; Zhang et al., 2007; Morisset et al., 2009; Bybee et al., 2014a,b). Previous geochronological data for the Ukrainian AMCG complexes (Amelin et al., 1994; Verkhogliad, 1995) indicated a long period of magmatism. However, these data were sparse and did not allow confident recognition of the

emplacement sequence and of the phases of magmatic activity. The temporal relationships between the main rock types had not been established, and correlation between the two Ukrainian AMCG complexes was hampered by the lack of data from one of them. Finally, it had been shown recently that mantle-derived dykes that vary in composition from kimberlite to tholeiitic dolerite, and which are widely distributed in the Ukrainian shield, are coeval with the AMCG complexes (Shumlyanskyy et al., 2012; 2016a; 2016b; Bogdanova et al., 2013).

Isotope data are used to shed light into the sources of the initial melts. Published data for the Ukrainian AMCG complexes are limited and signify a predominantly crustal source of the melts, with limited input of juvenile mantle material (Shumlyanskyy et al., 2006). However, isotope data for the silicic rocks was hitherto absent and ideas about relationships of basic and silicic members of the Ukrainian AMCG complexes in terms of their origin were highly speculative. In this paper we present extensive U-Pb geochronological and Hf isotope data on the two Palaeoproterozoic AMCG complexes located in the Ukrainian shield and sampled by the authors over the last decade. Our primary aim is to constrain the secular relationships between the main rock suites that compose the AMCG association and to shed light on their origins.

2. Geological setting

2.1. The Ukrainian shield

The Ukrainian shield hosts two AMCG plutonic complexes – the Korosten (KPC) and Korsun-Novomyrhorod (KNPC). The Korosten plutonic complex is in the North-Western domain of the Ukrainian shield, and the Korsun-Novomyrhorod complex is in the central part of the shield in the Ingul domain (Fig. 1). Both domains are dominated by orogenic granitoids

formed between c. 2080 and 2020 Ma (Shcherbak et al., 2008), while amphibolite facies supracrustal rocks compose large areas between the granitic intrusions, and also occur as variably-sized xenoliths within the latter. In both areas the Palaeoproterozoic crust prevails and Archaean rocks are virtually absent. However, there is a prominent difference in the isotope compositions of the Palaeoproterozoic rocks in the North-Western and the Ingul domains of the Ukrainian shield: the North-Western domain is dominated by juvenile metamorphic rocks and orogenic granites while their counterparts in the Ingul domain bear more "evolved" crustal isotope signatures and possibly originate from 200-300 M.y. older crustal precursors.

The North-Western domain was additionally affected by formation of the Osnitsk-Mikashevychi igneous belt at 2.0-1.97 Ga, which is thought to be an active continental margin that developed over the north-western margin of the already amalgamated Sarmatia and Volgo-Uralia segments of the East European Craton (Bogdanova et al. 2006; 2013; Shumlyanskyy, 2014). After c. 1.95 Ga the Ukrainian shield developed as a stable platform, and no orogenic events, deformation and strong metamorphism are known after that time. A thick, over 900 m, undeformed platformal sedimentary cover accumulated prior to the emplacement of the AMCG complexes, which are also undeformed and non-metamorphosed. The equant batholitic shape of these complexes further indicates an absence of any unidirectional stress during their formation.

2.2. Korosten plutonic complex (KPC)

The Korosten plutonic complex is one of the largest (about 10 400 km^2) and most typical examples of AMCG complexes in the world (Fig. 2). Granites occupy about 75 % of its area, and the rest is dominated by a range of basic rocks. The western, southern and eastern

contacts and several “windows” inside the KPC are composed of Palaeoproterozoic metamorphic rocks, granites and migmatites. Remnants of the platformal cover represented by Pugachivka sandstones, quartzites and schists occur as large xenoliths among the rocks of the Korosten complex and represent its ancient roof. To the north-west the KPC is bordered by the Bilokorovychi graben-syncline filled with platformal sediments (sandstones, siltstones, schists, conglomerates, and metabasalts) of the Topilnya Series, which according to the geological relationships is older than the KPC and is probably equivalent to the Pugachivka rocks. The U-Pb zircon age of the Bilokorovychi dyke swarm (Fig. 2) that cut sediments of the Topilnya Series is 1799 ± 10 Ma (Shumlyanskyy and Mazur, 2010). In its northern part, volcanic and terrigeneous rocks of the Ovruch Series fill the Ovruch and Vilcha basins and partly cover the KPC.

A large number of mantle-derived high-Ni tholeiitic dykes and several layered intrusions are known in the North-Western region of the Ukrainian shield, in the vicinity of the KPC. The available geochronological data indicate they were emplaced at 1790-1780 Ma (Shumlyanskyy et al., 2012; 2016a; Bogdanova et al., 2013).

The KPC embraces a number of granitic rocks that belong to the rapakivi group, and a suite of basic rocks that includes predominantly anorthosite and leucogabbronorite, and subordinate gabbro-noritic rocks. Other volumetrically minor rock types include monzonites, syenites, and monzonitic syenites. Basic rocks form sheet-like bodies, the largest of which occupies 1250 km^2, and vary in thickness from hundreds to thousands of metres. Such bodies are the gabbro-anorthosite massifs of Volynsky, Chopovychi, Fedorivka, Kryvotyn and Pugachivka, together with a number of smaller ones. Detailed field investigations have shown that the basic rocks of the KPC were intruded in a number of phases. Each phase corresponds to a specific rock assemblage called ‘rock series’ (Mitrokhin, 2001): early anorthositic (A_1), main anorthositic (A_2), early gabbroic (G_3), late gabbroic (G_4) and dyke (D_5).

The oldest known basic rocks of the KPC are high-alumina orthopyroxene megacryst-bearing anorthosite and leuconorite of the early anorthositic series (A_1). These occur mainly as xenoliths in younger basic and silicic rocks, but rather large bodies are also known. Rocks of the main anorthosite series (A_2) are the most abundant basic rocks of the KPC. They include leucocratic rocks varying from anorthosite to leucogabbronorite, which make up the main volume of the gabbro-anorthosite massifs. These rocks contain xenoliths of the A_1 rocks but in turn they are cut by later gabbroic intrusions and granites. Gabbronorite and leuco-gabbronorite that represent the early gabbro rock series (G_3) are known only in the southern part of the Volynsky massif. The late gabbro series (G_4) includes various rocks from leucogabbro to melagabbro and ultramafics that form layered intrusions and sheet-like bodies in association with A_2 massifs. G_4 rocks intrude all the large gabbro-anorthosite massifs of the KPC and they often contain economically significant apatite-ilmenite deposits, one of which (the Fedorivka layered intrusion) was described in detail by Duchesne et al. (2006). Ferromonzodiorite dykes that cut granitic rocks appear to represent the last manifestation of basic magmatism in the KPC, but recent geochronological data (Lubnina et al., 2009; Shumlyanskyy and Mazur, 2010; Shumlyanskyy et al., 2016a) indicate that ferromonzodiorite dykes (D_5) were emplaced throughout the history of the KPC. In general, ferromonzodiorite and quartz-ferromonzodiorite dykes are widespread in association with the Korosten AMCG complex. These dykes are often laden with plagioclase phenocrysts and are described in the literature under the names “plagioporphyrite” or “plagiophyric dolerite” or the local name “volynite”. The chilled margins of G_4 gabbroic massifs have similar to dykes compositions and share features that include the presence of variable amounts of K-feldspar, and correspondingly high K_2O contents (0.90-3.89 %). They also have high TiO_2 (1.91-3.77 %) and P_2O_5 (0.45-1.87 %) contents at relatively low Mg# (21-46). With respect to their chemistry, ferromonzodiorite dykes and chilled margins are broadly similar to rocks known as

jotunites in other AMCG complexes worldwide (Duchesne et al., 1985; Owens et al., 1993; Robins et al., 1997; Vander Auwera et al., 1998; Wiszniewska et al., 2002).

Granites of the rapakivi group are the dominant rocks at the current level of erosion, but characteristic coarse-grained wiborgitic rapakivi is rare. Medium-grained granites with sparse mantled ovoids are more common. Biotite-amphibole granites with fayalite and ferrous hedenbergite prevail near the contacts with basic rocks. Towards the central parts of the granitic massifs these turn into biotite-amphibole granite and then into amphibole-biotite granite. According to Esipchuk et al. (1990), emplacement of the KPC granites took place in a number of intrusive pulses (phases). The first and main phase of emplacement comprises the most abundant rapakivi-group granitoids, and the second phase is represented by minor stocks and dykes of biotite granite-porphyry. The third and final phase is represented by Li-F microcline-albite granite, which forms thin (<1.5 m) subvertical dykes among granites of the main and second intrusive phases (Shcherbakov, 2005). A group of hybrid rocks is located at contacts of the G_4 gabbroic intrusions with granites of the KPC. Gradual transformation of gabbronorite into monzonite, as well as of granite into granosyenite and quartz syenite, has been described and explained by mingling of high-temperature gabbroic melt with partly-crystallized granitic magma (Mitrokhin and Bilan, 2014).

2.3. The Korsun-Novomyrhorod plutonic complex

The Korsun-Novomyrhorod plutonic complex (KNPC) is an oval body elongated in the N-S direction with a total area of ~ 5 500 km^2. Granitic rocks occupy up to 76 % of the area and form two large massifs – the Korsun-Shevchenkivsky and Shpola (Fig. 3). The main variety of silicic rocks is coarse-grained rapakivi granite with numerous mantled ovoids (wiborgite). Granites with rare ovoids are less abundant and display gradual transitions into

wiborgite. Coarse-grained varieties are common in the internal parts of the granite massifs, and towards the margins coarse-grained granites are rimmed by a medium-grained variety. Aplite and pegmatite varieties of the biotite granite occur as veins cutting both rapakivi granite and basic rocks.

Basic rocks constitute c. 21 % of the area. Leucocratic rocks, i.e. anorthosite and leuconorite, are predominant and form four large massifs: the Novomyrhorod, Smila, Horodyshe and Mezhyrychi, as well as a number of smaller bodies. Mesocratic norite, gabbronorite and gabbro are far less abundant, and melanocratic gabbro and ultramafic rocks are very rare. Monzonitic rocks (monzonorite, monzodiorite, monzonite and syenite) cover about 3 % of the total area of the KNPC, and they usually occur at the contacts of granites against gabbroic rocks.

As in the KPC, rocks of the KNPC are closely associated with mafic (tholeiitic dolerite), ultramafic (picrite) and kimberlite dykes. Numerous fan-like dyke swarms are known south- and east-ward of the KNPC, but in spite of their wide areal distribution, these dykes do not cut rocks of the KNPC. Sparse geochronological data available for the dykes indicate emplacement at c. 1800 Ma. The possible relation of these mantle-derived dykes to a mantle plume, or to delamination of lithosphere caused by collision of Sarmatian and Fennoscandian segments of the East-European platform shortly before 1800 Ma, was discussed in details by Shumlyanskyy et al. (2016b). The intra-plate nature of this magmatism remains beyond doubt.

3. Methods

The U-Pb results were collected employing methods that include: thermal-ionisation mass-spectrometry (TIMS) on multigrain fractions of zircon and baddeleyite, secondary-ion

mass-spectrometry (SIMS) and laser-ablation ICP mass-spectrometry (LA-ICP-MS) carried out in-situ on individual zircon grains.

Most of our samples were taken from natural outcrops and artificial excavations (e.g. quarries) with reliable control of the sampled material. A few samples were taken from drill cores (Table 1) along intervals that varied from 2 to 20 m, depending on the availability of core material. Special attention was paid to collecting homogeneous rocks. Zircons and baddeleyites were separated from crushed whole rock samples, each weighing from 0.5 up to 30 kg, using conventional water table, heavy liquid and magnetic techniques. Subsequently, handpicked zircons were analysed by SIMS (Table 2), TIMS (Table 3) and LA-ICP-MS (Table 4) techniques. The TIMS analyses were made on multigrain fractions of zircon and baddeleyite. The samples were washed using HNO_3, H_2O and acetone, weighed on a microbalance and spiked with a mixed $^{205}Pb/^{235}U$ tracer. Dissolution of zircon was carried out with HF (+HNO_3) in Teflon bombs (Krogh, 1973) at 205˚C. The purified samples were loaded on zone-refined Re filaments with Si-gel and H_3PO_4 and measured on a TRITON spectrometer at the Swedish Museum of Natural History, Stockholm.

For the SIMS and LA-ICP-MS analyses the separated zircon crystals were mounted into a 25 mm epoxy puck and polished approximately half way through. Before isotope analysis, all zircon crystals were imaged using cathodoluminescence (CL) on a Hitachi SEM to clarify internal structures and to identify the portions most suitable for analysis. For the SIMS analysis the c. 1065 Ma Geostandard 91500 reference zircon (Wiedenbeck et al. 1995) was mounted along with the samples. The SIMS U–Th–Pb analyses were carried out using a large geometry Cameca IMS 1270 instrument at the Nordsim facility, Swedish Museum of Natural History, Stockholm. The analytical method follows that described by Whitehouse and Kamber (2005). The following procedures were fully automated: (a) pre-sputtering with a 25 mm raster for 120 s; (b) centring of the secondary ion beam in the 4000 mm field aperture; (c)

mass calibration optimization; and (d) optimization of the secondary beam energy distribution. Data reduction employed Excel® macros developed by M.J. Whitehouse.

The LA-ICP-MS techniques for U, Th, and Pb isotope analysis of zircon at the Museum für Mineralogie und Geologie (Senckenberg Museum of Natural History, Dresden), use a Thermo-Scientific Element 2 XR sector field ICP-MS coupled to a New Wave UP-193 Excimer Laser System. Each analysis consisted of a 15 s background acquisition followed by a 30 s data acquisition, using a laser spot-size of 25 μm. Raw data were corrected for background, common Pb, laser induced elemental fractionation, instrumental mass discrimination, and time-dependant elemental fractionation of Pb/Th and Pb/U using an Excel® spreadsheet program developed by Axel Gerdes. U and Pb contents and Th/U ratios were calculated relative to the GJ-1 zircon standard and are accurate to approximately 10%.

In all methods described above the common lead correction, when needed, was done using the measured ^{204}Pb signal and the modern (i.e. 0 Ma) Pb isotope composition (Stacey and Kramers, 1975). The reported discordance refers to the position of data points in relation to the concordia curve in conventional ^{207}Pb/^{235}U–^{206}Pb/^{238}U space. Decay constants used follow the recommendations of Steiger and Jäger (1977). Age calculations were performed using the routines of ISOPLOT 4.15 (Ludwig, 2012).

To ensure that applied methods of U-Pb dating produce comparable results, one sample of granite (sample 05-C1, Susly quarry) was analysed by all three methods. Results of dating (2059 ± 5 Ma) are identical within error.

Hf isotope analyses were performed at Bristol University, UK. The data were acquired with a Thermo-Scientific Neptune multicollector inductively coupled plasma mass spectrometer (ICP-MS) coupled to a New Wave 193 nm ArF laser ablation sampling system operating at 4 Hz and using a 50 mm spot size over a 60 s ablation period. The Yb isotope compositions of Segal et al. (2003) were adopted for interference corrections which are done

by determination of the Yb mass bias by measuring $^{173}Yb/^{171}Yb$ during the run, and calculating $^{176}Yb/^{177}Hf$ using the natural $^{176}Yb/^{171}Yb$ ratio. The relatively minor Lu correction was performed by measuring ^{175}Lu and using $^{175}Lu/^{176}Lu=0.02655$ (Vervoort et al., 2004), assuming that the mass bias behaviour of Lu is analogous to that of Yb Kemp et al. (2009).

Data for unknowns were collected along with Plešovice, Temora and 95100 standards. $^{176}Hf/^{177}Hf$ initial values were calculated using the ^{176}Lu decay constant of Söderlund et al. (2004). Depleted mantle (Chauvel and Blichert-Toft, 2001), and chondritic (Bouvier et al., 2008) parameters were used for model age calculations.

Some of the zircons from the Ukrainian AMCG complexes had high $^{176}Yb/^{177}Hf$ ratios (up to 0.12) that required robust correction procedures to deal with the isobaric interference on ^{176}Hf. Analyses of synthetic zircon doped with Hf and REE carried out at Bristol University (Fisher et al., 2011), using the same method as the one applied here, demonstrated that even such high Yb isobaric interferences can now be satisfactorily corrected.

4. Geochronological data

4.1. The Korosten plutonic complex (KPC)

4.1.1. Previous results

Table 1 summarizes previous age results with relevance for this study, together with the new results presented here. Rocks of the A_1 (early anorthosite) series have been dated by Amelin et al. (1994) and Verkhogliad (1995) using the U-Pb method on zircon and baddeleyite. A coarse-grained anorthosite on the right bank of the river Uzh, near the village Pugachivka (for sample and locality numbers, see Table 1) yielded ages of 1800.0 ± 1.3 Ma for zircon and 1794 ± 7 Ma for baddeleyite. Xenoliths of the early anorthosite host within the

main anorthosite series from the Ignatpil quarry yielded a concordant U-Pb zircon age of 1789 ± 2 Ma. Finally, a sub-concordant zircon age of 1784 ± 3 Ma was obtained for a xenolith of anorthosite enclosed in an A_2 anorthosite at the Granitne quarry. Large anorthosite bodies of the main anorthosite series (A_2) had been previously dated at two localities within the Volynsky massif. Zircon dating of anorthosite from the Holovino quarry yielded a concordant age of 1758.1 ± 1.0 Ma, and the baddeleyite age was 1760.6 ± 0.7 Ma. Zircons from the Turchynka anorthosite yielded a concordant age of 1758.0 ± 1.8 Ma. Numerous gabbroic massifs of the G_4 rock series were, until recently, represented by a single concordant zircon age of 1758.8 ± 0.9 Ma for gabbro in the Buky quarry. Amelin et al. (1994) and Verkhogliad (1995) also reported a concordant age of 1761 ± 2 Ma for zircons from a plagiophyritic dyke that crops out near Pugachivka village, where it cuts granites of the KPC. Ferromonzodiorite from the Bilokorovychi dyke swarm yielded a zircon age of 1799 ± 10 Ma (Shumlyanskyy and Mazur, 2010). Shumlyanskyy et al. (2016a) report results of U-Pb baddeleyite dating of the Rudnya Bazarska dyke, which at 1000-1500 m wide, is one of the largest dykes associated with the KPC (Fig. 2). An unconstrained regression yielded an upper intercept age of 1793 ± 6 Ma. Finally, the youngest known subvolcanic ferromonzodioritic sill intrusion is exposed in the Bondary quarry where it cuts granites of the KPC. The U-Pb zircon age of this rock is 1751 ± 12 Ma (Lubnina et al., 2009).

In spite of the fact that granitic rocks prevail at the surface of the KPC, only three samples had previously been dated by the U-Pb method. Zircons from the rapakivi granite in the Kyivshlyakhobud quarry near the city of Malyn were dated by Shcherbak et al. (1989), Amelin et al. (1994), and Verkhogliad (1995); a combination of all of their data yields an age of 1765 ± 5 Ma. A second sample was taken at the Lezniki granite massif and gave an age of 1752 ± 16 Ma. A third granite sample is from a thin vein (dyke) of granite porphyry that cuts schists of the Bilokorovychi basin, and its age is 1781 ± 3 Ma (Amelin et al., 1994). Basic

(basalt) and silicic (rhyolite) volcanic rocks occur in the basal parts of the Ovruch and Vilcha basins. Some rhyolite crops out at the surface and was the subject of a detailed geochemical and geochronological study (Shumlyanskyy and Bogdanova, 2009). Geochemically these rocks closely resemble granites of the KPC, and their zircon U-Pb age (1761 ± 13 Ma) also indicates a tight genetic relationship with silicic plutonic rocks of the KPC.

There are also a number of smaller intrusions located up to several tens of kilometres from the main intrusive body of the KPC. One of these intrusions is the Yastrebetsky syenite massif (Fig. 2). The U-Pb SIMS zircon age of these syenites is 1772 ± 6 Ma (Sheremet et al., 2012) which also indicates a link to the KPC.

4.1.2. New U-Pb age results

The details of the analytical methods are given in Supplementary Appendix A.

The early anorthositic series (A_1) is represented by sample no. 68 that was collected at quarry #6 near the Granitne village close to the city of Malyn. It occurs as a large xenolith of A_1 anorthosite within the A_2 anorthosite. Zircons are colourless to slightly pinkish, transparent, and up to 0.2 mm long. Grains are equant and prismatic, with a few of them being elongated. Crystals are weakly zoned, and zoning is oscillatory, concentric or sectorial. On CL images grains are rather dark with only a few of them having bright external mantles (Fig. 4). Zircons were dated by SIMS and yielded concordant or nearly concordant results (Table 2); the weighted average $^{207}Pb/^{206}Pb$ age is 1778 ± 9 Ma, while the upper intercept age is 1781 ± 8 Ma (Fig. 5).

Anorthosites of the main anorthosite series (A_2) contain locally abundant pegmatitic pods that represent clusters of the residual liquid left after anorthosite crystallization (Shumlyanskyy and Zagnitko, 2011). We have analysed zircons from pegmatites that occur in the Paromivka, Horbuliv and Syniy Kamin quarries, all hosted within A_2 anorthosites of the

Volynsky massif. Four multi-grain TIMS results were obtained for zircons from pegmatites of the Paromivka quarry, three multi-grain results for the Syniy Kamin pegmatites, and five multi-grain TIMS results and five SIMS spots for pegmatites of the Horbuliv quarry (Tables 2, 3). Zircons from all of these pegmatite bodies are very similar and occur as large, >0.2 mm, prismatic, elongated or flattened crystals. The zircons are transparent, colourless or slightly pinkish, and luminescence is very weak to absent (Fig. 4). The new ages indicate that pegmatites of the Paromivka quarry crystallized at 1757 ± 3 Ma (weighted average $^{207}Pb/^{206}Pb$ age, MSWD = 0.94, and the upper intercept is 1757 ± 4 Ma if the lower intercept is anchored at 0 Ma). Similarly, the upper intercept ages of zircons from the Syniy Kamin and Horbuliv quarries are 1756 ± 4 Ma and 1754 ± 4 Ma (ages obtained with the lower intercept anchored at 0 Ma, Fig 5). The combined weighted average $^{207}Pb/^{206}Pb$ age for all results obtained for the three different pegmatite bodies is 1758 ± 4 Ma. We accept this age as the time of crystallization of the pegmatites in the Volynsky gabbro-anorthosite massif. It corresponds to the previously obtained age of their host anorthosites (1758 ± 2 Ma, Verkhogliad, 1995).

Sample 10-03 was taken at the same quarry as sample no. 68, and it is an anorthosite of the Fedorivka anorthosite massif (which should not be confused with the Fedorivka gabbro layered intrusion) that is the third largest anorthosite massif in the KPC (Mytrokhyn et al., 2003; Fig. 2). This anorthosite belongs to the A_2 rock series and it contains numerous xenoliths of the A_1 anorthosite dated by Verkhogliad (1995) and in this work (sample no. 68). From sample 10-03 five fractions of baddeleyite have been dated (Table 3), most of which yielded concordant or sub-concordant U-Pb (TIMS) results with one result being reversely discordant (Fig. 5). The upper intercept of the discordia line (anchored at 0 Ma) yielded an age of 1771.5 ± 0.8 Ma, and the weighted average $^{207}Pb/^{206}Pb$ age is 1771.6 ± 1.5 Ma. This age is younger than that of xenoliths hosted by this rock (1784 ± 3 and 1781 ± 8), but appropriately older than the age of the A_2 anorthosites (~1758 Ma) of the Volynsky massif.

Special attention was paid to rocks of the late gabbroic series (G_4), as these often contain economic apatite-ilmenite ores. Sample 599 is an olivine gabbro of the Fedorivka layered intrusion. Two non-magnetic multigrain fractions of zircons differing in size (<0.1 mm and 0.1-0.2 mm) and four fractions of baddeleyite were dated by TIMS. Zircons are almost colourless to slightly brownish, transparent, and commonly containing minor inclusions. Grains are elongated and prismatic with well-developed pyramidal tips, and on CL images the zircons display complex irregular zoning (Fig. 4). All the results from this sample are concordant to sub-concordant (discordance <3 %, Table 3, Fig. 5), and the combined zircon and baddeleyite age is 1761.9 ± 1.6 Ma (upper intercept age).

Sample 03-D24 is of olivine gabbronorite from the Pivnichna Slobidka G_4 massif. Zircons from this rock are almost equant and about 0.1 mm in size. Prismatic facets are absent or poorly developed, and the crystals are transparent, colourless to slightly brownish. Zoning is apparent on CL images as a thin dark mantle surrounds the grey main portion of the grains (Fig. 4). Six crystals were analysed by SIMS, five of them were <4 % discordant, while one grain yielded a significantly discordant (23 %) result (Table 2, Fig. 5). The age of crystallization calculated using all 6 results is 1763 ± 8 Ma (upper intercept age) whereas the weighted average $^{207}Pb/^{206}Pb$ age is 1763 ± 4 Ma.

Olivine monzodiorite of the Torchyn G_4 massif was sampled at the Torchyn quarry (sample 03-D18). Zircons are slightly elongated and di-pyramidal, and prismatic facets are virtually absent. Crystals are transparent, but slightly brownish. On CL images these zircons occur as dark grains with very weak simple zoning (Fig. 4). In total, five grains were dated by SIMS; three of them yielded sub-concordant (<4 % of discordancy) results, while two crystals are significantly discordant (Table 2, Fig. 5). The age of the upper intercept of the regression (anchored at 0 Ma) for all five grains is 1756 ± 5 Ma, while the weighted average $^{207}Pb/^{206}Pb$ age is 1757 ± 9 Ma.

Sample 289/197 is a gabbro of the Davydky massif that is rather atypical for the KPC. It is located in the extreme north-eastern corner of the KPC (Fig. 2) and it occurs as a rounded body that occupies an area of 30 km^2. Unlike other gabbroic bodies in the KPC, the Davydky massif displays a clear fractionation from gabbro to syenite. Two fractions, with 2-3 baddeleyite grains in each, and one single-grain fraction were analysed by TIMS for U-Pb isotopes. All the results are concordant and very consistent (Table 3, Fig. 5) and yield an age of 1789.8 ± 1.5 Ma (lower intercept anchored to 0 Ma).

In addition, our intention was also to expand the geochronological dataset for silicic rocks of the KPC, which had previously lacked adequate attention. Two of the granite samples were collected at the extreme northern part of the KPC, close to the contact with country rocks; these granites were recovered by drilling under the thin sedimentary cover. Zircons from sample 503/105 are euhedral and elongate, with well-developed prismatic and di-pyramidal facets; crystals are transparent to semi-transparent, pinkish and commonly loaded with numerous solid and fluid inclusions. On CL images these zircons display pronounced zoning (Fig. 4). U-Pb isotopic analyses of these zircons were carried out by LA-ICP-MS; seven grains were analysed, of which three yielded concordant results, whereas the remaining four are 6 to 30 % discordant (Table 4, Fig. 5). The age calculated for the three concordant grains is 1810 ± 14 Ma.

Zircons from the second granite sample (75/146) are euhedral and short-prismatic, with well-developed prismatic and di-pyramidal facets. Optically these crystals are grey, transparent to semi-transparent, and commonly exhibit pronounced sectorial zoning revealed by accumulations of brownish dust-like inclusions. Fluid inclusions are present, but they are not as abundant as in zircons from sample 503/105. On CL images these zircons are predominantly dark-grey, with weak concentric zoning (Fig. 4). Among six grains dated by

LA-ICP-MS, two yielded concordant results (concordia age = 1817 ± 15 Ma) whereas the others are 8 to 21 % discordant (Table 4, Fig. 5).

The third granite sample (06-BG48) is from fine-grained granite at the Bondary quarry in the northern part of the KPC. Zircons from this rock are transparent, colourless to slightly brownish, and commonly exceed 0.25-0.30 mm in size. Their shape varies from prismatic to elongated prismatic with well-developed pyramidal tips. Solid inclusions are quite common, and zoning is virtually absent (Fig. 4). The Bondary granite was dated by means of SIMS on single zircon grains. All five analysed grains yielded rather discordant results, with an upper intercept at 1780 ± 6 Ma (Table 2, Fig. 5).

Sample 53-7 is a typical wiborgite from an outcrop near the Myrne village. The zircons occur as irregular fragments (0.2-0.5 mm) of even larger crystals, colourless and transparent, and weakly zoned on CL images (Fig. 4). Concordant U-Pb data were obtained (Table 2, Fig. 5), and the $^{207}Pb/^{206}Pb$ weighted average age is 1763 ± 6 Ma.

Zircons from another rapakivi-group granite (sample 95005), taken from an abandoned quarry in the Huta Potiivka village, are prismatic, 0.3 to 0.5 mm in size, colourless, transparent, with simple concentric zoning (Fig. 4). Seven SIMS analyses were carried out on five zircon grains (core and outer parts were both analyzed in two grains) that yielded nearly concordant results (Table 2, Fig. 5). The upper intercept age is 1767 ± 7 Ma, and the $^{207}Pb/^{206}Pb$ weighted average is 1765 ± 3 Ma.

Granite sample 168-1 is a subalkaline biotite granite-porphyry that crops out near the Hamarnya village. Here, granites form small stocks that cut rapakivi granites of the main emplacement phase and belong to the second emplacement phase recognized by Esipchuk et al. (1990). Zircons from this sample are prismatic and elongated with well-developed di-pyramidal terminations. Grains are transparent, colourless to pale pinkish, often cracked and they contain sparse fine inclusions. Three multigrain fractions were dated by the TIMS

method and yielded discordant results (Table 3, Fig. 5) with an upper intercept age of 1758 ± 5 Ma.

Finally, zircons from a granite sample (03-D1) representing veins of Li-F microcline-albite granite exposed in the Andriivka village have been analysed by SIMS. These rocks belong to the last known manifestation of magmatic activity within the KPC. The zircons are well-developed, prismatic with poor pyramidal facets, transparent, and slightly pinkish. Grain size varies between 0.10 and 0.15 mm and CL images are very dark and do not reveal any zoning (Fig. 4). All grains except one are very discordant. The concordia age of the Andriivka granite is 1743 ± 5 Ma (Table 2).

The two samples represent the suite of monzonitic and syenitic rocks. One is a granosyenite (71-9) that was taken at Buky village. Zircons are prismatic, predominantly elongated, commonly with curved irregular outlines, and the length of the grains varies from 0.2 to over 0.5 mm. Zonation is very weak and was seen in a few grains (Fig. 4). Five of the six results of SIMS dating were concordant or nearly-concordant, with one result being strongly discordant (Table 3, Fig. 5). The obtained upper intercept age is 1764 ± 3 Ma and the weighted average $^{207}Pb/^{206}Pb$ age is 1763 ± 4 Ma.

The second sample (71-1M) is a monzodiorite (marginal facies) from the Buky massif. Zircons extracted from this rock are quite large (c. 0.5 mm), transparent and colourless, prismatic, with poorly developed di-pyramidal tips, and CL-imaging reveals simple concentric zoning (Fig. 4). Five zircon grains (with two analyses carried out on internal and marginal parts of the same grain) yielded sub-concordant SIMS results (Table 2, Fig. 5); a regression yielded an upper intercept age of 1761 ± 5 Ma, whereas the weighted average of $^{207}Pb/^{206}Pb$ ages is 1761 ± 4. These ages are within error of the 1758.8 ± 0.9 Ma age obtained previously for a gabbronorite specimen from the same massif (Amelin et al., 1994; Verkhogliad, 1995).

4.2. The Korsun-Novomyrhorod plutonic complex (KNPC)

4.2.1. Previous results

The understanding of the geochronology of the KNPC has been significantly improved in recent years. Dovbush et al. (2009) reported U-Pb zircon ages of anorthosites of the Novomyrhorod massif (1750.2 ± 0.9 Ma) and of an olivine-amphibole monzonite dyke (1753 ± 7 Ma). Shestopalova et al. (2010) dated allanites from the wiborgites, one of which was sampled at the Sivach quarry near the city of Korsun-Shevchenkivsky and yielded an age of 1753.9 ± 0.8 Ma. Another sample from the Prudyansky quarry near the city of Vasylkiv yielded an age of 1753.7 ± 1.1 Ma. A similar age (1752 ± 12 Ma) was obtained by Shcherbak et al. (2008) for wiborgite from a quarry in Tashlyk village. Ponomarenko et al. (2011) reported a U-Pb zircon age (1758 ± 3 Ma) for a granite of the Ruska Polyana massif from the extreme north-eastern part of the KNPC.

The most recent zircon U-Pb ages for the KNPC rocks were reported by Shestopalova et al. (2013): 1747 ± 4 Ma for wiborgite of the Shpola massif from the Prudyansky quarry; 1748 ± 4 Ma for granite from the same quarry; 1750.1 ± 1.2 Ma for troctolite of the Horodyshe massif sampled at the Voronivka village; 1749.0 ± 0.5 Ma for porphyritic norite taken from the same massif in the Khlystunivka village; and finally 1739 ± 3 Ma for leuconorite from the same locality. Hence, all the published ages for the KNPC fall within a narrow time interval ~1754-1740 Ma and indicate close temporal relationships between the basic and silicic rocks.

Shestopalova et al. (2014) presented geochronological indications of the possible presence of older rocks in the KNPC. These authors investigated zircons from a xenolith of white (altered) anorthosite that was found within anorthosite of the main phase, in the

Kamyanka village. Zircons in the xenolith are variable in terms of both their appearance and age (the $^{207}Pb/^{206}Pb$ ages vary from 1744 to 1806 Ma).

4.2.2. New U-Pb age results

We have dated zircons from six rocks of the KNPC as outlined below. The Khlystunivka quarry is in the Horodyshe massif (Fig. 3), and it exposes a medium-grained quartz monzonite, which in the western part of the quarry is cut by a thick (20-30 m) sheet-like syenite body. Contacts between these rocks are usually sharp and uneven, without any evidence of alteration. However, gradual transitions of one rock type into another were also documented. A quartz monzonite (sample 06-BG4) contains prismatic to elongate zircon grains with well-shaped prismatic and pyramidal facets. Crystals are large, up to 0.3 mm in length, and euhedral. Zoning is visible both on CL images (Fig. 6) and optically. Core portions of the grains are colourless and transparent. The marginal parts are brownish to dark brown, and they are often cracked and contain mineral inclusions. Three individual grains were analysed from this sample (Table 2) by SIMS. The results are nearly concordant, and a regression line (anchored at 0 Ma) yielded an upper intercept age of 1746 ± 9 Ma (Fig. 7), while the weighted average $^{207}Pb/^{206}Pb$ age is 1746 ± 23 Ma.

Zircons from a quartz syenite (sample 06-BG5) in the Khlystunivka quarry display an equant to elongated prismatic habit with well-developed prismatic facets and complex di-pyramidal tips. Crystals are brownish, cracked and contain mineral inclusions. The core parts are intensively coloured while marginal portions are commonly colourless and transparent; CL images reveal complex concentric zoning (Fig. 6). All five individual grains analysed in this sample fall on a regression line that intersects the concordia at 1748 ± 7 Ma (Fig. 7).

The Nosachiv norite body is part of the Smila anorthosite massif (Fig. 3). The main portion of the body is composed of olivine-apatite-ilmenite and olivine-ilmenite norite

(sample 2006), and there is subordinate ilmenite norite with a minor amount of olivine and apatite (sample 2008). Host rocks to the Nosachiv body are anorthosites of the Smila massif (sample 2004).

Zircons from sample 2006 occur as fragments (0.2-0.3 mm) of even larger prismatic crystals. They are colourless to slightly brownish and weakly luminescent, zoning is weak and irregular (Fig. 6), and fine mineral inclusions are common. All five analyzed grains yielded nearly concordant SIMS results (Table 2, Fig. 7), and the weighted average $^{207}Pb/^{206}Pb$ age is 1756 ± 4 Ma. The addition of data for one baddeleyite multigrain fraction (TIMS) to the zircon regression results in an upper intercept age of 1755 ± 6 Ma.

Zircons from sample 2008 are texturally indistinguishable from those in sample 2006 (Fig. 6), and they also yield similar U-Pb zircon ages; six analyzed grains yielded near-concordant ages with a weighted average $^{207}Pb/^{206}Pb$ age of 1757 ± 4 Ma (Fig. 7). To improve the precision of the SIMS zircon ages we analysed baddeleyites from the same sample, but they yielded different ages with two baddeleyite fractions having a weighted average $^{207}Pb/^{206}Pb$ age of 1766.4 ± 1.8 Ma (Table 3). These are the only baddeleyite results that differ significantly from the zircon data, and since the specimen was taken from a drill hole as a set of sub-samples collected along c. 20 m long interval, it is possible that data represent two different norite rock bodies, one of which was dated by zircon, and another by baddeleyite.

Zircons from the anorthosite sample 2004 are large (up to 0.5 mm), prismatic to equant, with well-shaped prismatic facets and suppressed pyramidal ones. The crystals are colourless to slightly brownish, and a few grains are bright brown. Mineral inclusions distributed along the long axis of the crystals are quite common, and grains are usually unzoned and non-luminescent (Fig. 7). All except one of the six grains yielded nearly concordant results. The upper intercept age is 1754 ± 4 Ma, and a weighted average $^{207}Pb/^{206}Pb$ age for nearly concordant results is 1756 ± 4 Ma.

The possible presence of an older generation of anorthosites in the KNPC was mentioned previously in the context of published age results from a xenolith of older anorthosite enclosed in anorthosite of the main phase (sample KN-1/2, Shestopalova et al., 2014). In order to shed further light on this issue we dated three single zircon crystals separated from the same xenolith. The regression line through the (TIMS) data is quite imprecise (upper intercept is 1755 ± 60 Ma, MSWD = 23) in accordance with the noted heterogeneity of zircons in this sample (Shestopalova et al., 2014). However, six of the ten results from Shestopalova et al. (2014) plot close to the regression line defined by our three data points. If data that seemingly define a single discordia (n=9) are combined, a more precise upper intercept of 1756 ± 7 Ma is obtained, which is within error of the age of the anorthosite (1750.2 ± 0.9 Ma) that hosts this xenolith. Four zircon fractions dated by Shestopalova et al. (2014) yielded even older ages with two concordant points as old as 1801 ± 10 Ma (Fig. 7).

4.3. Summary of geochronology of the Ukrainian AMCG complexes

The new geochronological data provide a new understanding of the emplacement history of the Ukrainian AMCG complexes, the KPC and KNPC, and the basis for a model of their formation (see Fig. 9 and the associated discussion). Previously, only the early anorthosite had been dated, and the new data indicate that formation of the KPC started at c. 1815 Ma with the emplacement of granites in its northern part. This was shortly followed by the assemblage of silicic and basic rocks at 1800-1780 Ma, and it is now clear that main phase granites predominantly preceded emplacement of the basic intrusions. We have established that formation of the large anorthosite massifs of the main emplacement phase within the KPC continued over a period of 10 M.y. Our new data further highlight that the formation of

the KPC was accompanied by the emplacement of numerous ferromonzodioritic dykes and sills (1800 to 1750 Ma). These geochronological results are in agreement with field relationships which suggest the repeated emplacement of dykes.

With respect to the KNPC the new data are consistent with previously published results. The KNPC is slightly younger than the KPC, and it was also emplaced during a single pulse of magmatic activity that lasted for 10 M.y.

5. Lu-Hf isotope results

Hafnium isotope ratios were measured in nine zircon samples selected as representative of the rocks of the KPC, and six samples as representative of the rocks of the KNPC. Hafnium isotopes were measured at the same spots that were analysed previously for U-Pb ages by SIMS, and all εHf values were back-calculated to their U-Pb ages (Table 5).

5.1. The Korosten plutonic complex (KPC)

The results of the Hf isotope measurements are reported in Table 5 and displayed graphically in Fig. 8. The average εHf value in zircons from the early anorthosites (A_1 series, sample #68) is 0.1 ± 0.4; this value is similar to values (0.0 ± 0.3) for zircons from pegmatites (samples Parom and Horbul) in anorthosites of the main (A_2) series. Hafnium in zircons from the ilmenite-bearing gabbroic intrusions (G_4 series) is slightly more radiogenic: the εHf value for zircon from the Torchyn massif (sample 03-D18) is 0.1 ± 1.3 and from the Pivnichna Slobidka massif (sample 03-D24) is 0.4 ± 0.4. Hafnium in zircons from the gabbro of the Fedorivka ilmenite deposit (sample 599) is less radiogenic with εHf = -0.8 ± 1.4. Zircons from the early granites of the northern part of the KPC (Bondary quarry, sample 06-BG48)

have εHf values -1.2 ± 1.0, and εHf in zircons from rhyolite of the Ovruch basin (sample 06-HB7) is -1.3 ± 0.3. A ferromonzodioritic sill that crops out in the Bondary quarry (sample 06-BG47) contains zircons with the lowest εHf of -3.5 ± 0.5.

5.2. The Korsun-Novomyrhorod plutonic complex (KNPC)

The hafnium isotope ratios in zircons from rocks of the KNPC are less radiogenic than those of zircons in the KPC. For instance, εHf in zircons from anorthosites of the Smila massif (sample 2004) is -3.1 ± 0.5, and similar Hf isotope compositions are obtained for zircons in olivine-ilmenite norite of the Nosachiv gabbroic massif (εHf = -3.0 ± 0.5, sample 2006), and the ilmenite norite of the same massif (-3.5 ± 0.8, sample 2008). The εHf in zircons from wiborgite near the city of Korsun-Shevchenkivsky (sample 06-BG1) is -2.4 ± 0.9, whereas the value from quartz monzonite in the Khlystunivka quarry (sample 06-BG4) is -2.8 ± 0.8, and from quartz syenite in the same quarry (sample 06-BG5) is -2.9 ± 0.9.

Overall the εHf values within the Korosten complex show relatively little variation, as so those from the KNPC, but the εHf values in the KPC are slightly more radiogenic than those in the KNPC (Fig.8).

6. Discussion

6.1. Emplacement history

6.1.1. The Korosten plutonic complex (KPC)

Our new U-Pb zircon and baddeleyite age data, integrated with previous data for the KPC indicate that the formation of this plutonic complex was more complicated and

prolonged than was thought previously. Formation started with emplacement of granites in its northern part at c. 1815 Ma (Table 1, Fig. 9), although there has been some uncertainty as to whether these rocks directly belong to the KPC or are part of a suite of granites that reflect collision between Fennoscandia and Volgo-Sarmatia. However, their chemical and isotope compositions, which will be discussed in a separate paper, are indistinguishable from the typical KPC granites, and so they are considered to belong to the KPC. The oldest basic rocks of the KPC belong to the early anorthosite (A_1) series that crystallized between c.1800 and 1780 Ma. Mineralogical data indicate that these rocks were crystallized at lower crustal levels (9.6-13.3 kbar, or 30-40 km), and they were brought to the surface as xenoliths by subsequent magmas (Mitrokhin et al., 2008). Data presented by Shumlyanskyy and Mazur (2010), and Shumlyanskyy et al. (2016a) indicate that at least some of the KPC-related ferromonzodioritic dykes intruded into the host rocks at 1800-1790 Ma. New ages obtained for the granites of the Bondary quarry (1780 Ma) and for the gabbro of the Davydky massif (1790 Ma) suggest that some of the granites and gabbroic massifs were emplaced simultaneously with A_1 anorthosites. Thus, a whole spectrum of rocks (anorthosite, gabbro, ferromonzodiorite and granite) was formed during the first pulse of magmatic activity at 1815-1780 Ma. It should be stressed (i) that this earliest stage of the KPC formation coincides in time and space with emplacement of the mantle-derived high-Ni tholeiites (Shumlyanskyy et al., 2012; 2016a; Bogdanova et al., 2013), and (ii) the vast majority of the KPC rocks presently exposed at the surface were formed subsequently in a much shorter time period between c. 1768 and 1755 Ma as indicated by the ages summarized in Table 1 and Fig. 9.

- Large anorthosite bodies of the main anorthosite (A_2) series: anorthosites of the Volynsky massif crystallized between c. 1761 and 1758 Ma, while residual melts, represented by pegmatitic pods, crystallized at c. 1758 Ma. These anorthosite bodies, which are up to 2 km thick and cover up to 1000 km^2, solidified within a few million years. The age of c. 1771

Ma obtained for anorthosites of the Fedorivka massif signifies that formation of large anorthosite massifs was a complex and protracted process, which continued from c. 1770 to 1758 Ma.

- Numerous gabbroic intrusions (G_4 series) in the inner and marginal parts of the A_2 anorthosite massifs were formed between 1763 and 1757 Ma; their age is indistinguishable (within error) from that of the host anorthosite.

- The ferromonzodioritic dykes were intruded at c. 1761 Ma.

- All rapakivi-group granites and syenites that belong to this pulse of magmatic activity have ages that fall within a narrow interval of 1765-1762 Ma. These ages contradict the widely held opinion that the rapakivi-group granites are younger than the basic rocks.

- Small bodies of biotite granite-porphyry were intruded into rapakivi-group granites at c. 1758 Ma, i.e. simultaneously with the anorthosites and gabbros.

- Finally, rhyolites of the Ovruch basin were erupted at 1761 ± 13 Ma.

After c. 1758 Ma magmatic activity within the KPC gradually ceases. The youngest rocks of the complex are represented by the late subalkaline granites of the Lezniki massif and veins of Li-F microcline-albite granites (1752 ± 8 Ma and 1742 ± 9 Ma, respectively).

6.1.2. The Korsun-Novomyrhorod plutonic complex (KNPC)

The KNPC is similar to the KPC in many major features, but the ranges of U-Pb ages are different (Fig. 9). In the KPC, c. 1800 Ma zircons were found in a xenolith of altered anorthosite (Shestopalova et al., 2014) and 1766 Ma baddeleyite in a norite of the Nosachiv intrusion, but the implications of these results are uncertain. The older ages (~ 1800 Ma) obtained for zircons in the xenolith may correspond to the time of initial crystallization of the early generation of anorthosites. The oldest known rocks of the KNPC with well established ages are the anorthosites and norites emplaced at c. 1757-1754 Ma (Table 1, Fig.9).

Anorthosites of the Novomyrhorod and Smila massifs and various rapakivi units of the KNPC formed between 1754 and 1750 Ma, whereas the youngest dated rocks of the KNPC are monzonites and syenites of the Khlystunivka quarry that crystallized at c. 1748-1740 Ma. Still younger ages (1739 ± 3 Ma) obtained for leuconorite collected in the Khlystunivka quarry (Shestopalova et al., 2013) require further confirmation.

Thus, rocks of the KNPC appear slightly younger than the main intrusive phase of the KPC. Another observation, noted in both areas, is that most of the silicic and basic rocks were intruded within a time interval of around 10 M.y.

6.2. Duration of the AMCG magmatism and its relation to the coeval mantle-derived mafic melts

The KPC and KNPC occur as large igneous bodies (over 10 400 and 5 500 km^2, respectively) that extend down to mid-crustal levels, and perhaps to the mantle-crust boundary as evidenced by an extensive set of geophysical data (Bogdanova et al., 2004). Taking into account the geophysical imaging, the volume of the Korosten plutonic complex can be estimated between 60 000 and 120 000 km^3. Considering the duration of magmatic activity in the KPC over a total age range of c. 70-60 M.y., but grouped into two main pulses, the average rate of magma production was equal to 1 000 – 2 000 km^3/M.y., perhaps reaching 6 000 – 12 000 km^3/M.y. at peak periods. The peak rate is 2-3 orders of magnitude less than the magma production rate in continental flood basalt provinces, which are erupted over much shorter time periods, and some 10 times less than the magma eruption rate in oceanic islands (White et al., 2006 and references therein). However, the estimated rate of magma production is broadly similar to the eruption rates in continental rifts and continental hotspots (White et

al., 2006). Such rates also correspond to the emplacement rates of some other AMCG complexes (Amelin et al., 1997).

Formation of such large magma volumes implies that significant additional heat was available for prolonged periods of time. It should be noted that both Ukrainian AMCG complexes were emplaced into stable continental crust, some 150-200 M.y. after the last orogenic event. However, their formation was accompanied by emplacement of a wide range of mantle-derived melts that includes tholeiites, subalkaline mafic and alkaline ultramafic varieties that are similar to within plate rocks elsewhere (Ernst, 2014), in contrast to the initial ferromonzodioritic melts for the KPC which have less of a within-plate signature. On diagrams showing fields of basalts from different tectonic settings (Condie, 2005; Fig. 10), most of the tholeiitic dykes plot in the fields of ocean plateau and ocean island basalts close to the primitive mantle. In contrast, most of the KPC ferromonzodiorites plot in the field of arc-related basalts and gravitate towards the upper continental crust that is consistent with a prevalence of material from pre-existing continental crust.

Mantle-derived melts were intruded throughout the Sarmatian segment of the East European craton both in the Ukrainian shield and the Voronezh crystalline massif. Most of these dykes were intruded between 1770 and 1790 Ma (Chernyshov et al., 2001; Bogdanova et al., 2013; Shumlyanskyy et al., 2012; 2016b) which is perhaps longer than might be expected in many models of magmatism linked to the emplacement of a mantle plume. However, while some plume-related large igneous provinces are emplaced in extremely short periods of less than 2 M.y. (e.g. the Siberian Trap), there are other plume-related events which are emplaced in multiple pulses over a longer period of time (e.g. the 1115-1085 Ma Keweenawan large igneous province of the Great Lakes region of North America; Ernst, 2014). The dykes correspond to the earlier stages of KPC evolution, but somewhat postdate initiation of magmatism within the KPC. Nonetheless, the presence of relatively hot mantle,

which might be attributed to a mantle plume but that is difficult to establish, appears to be required for the generation of the large volumes of magma observed, and the heating of the lower crust and formation of ferromonzodioritic melts.

Bogdanova et al. (2013) challenged the relationship of dykes in the Ukrainian shield (and AMCG complexes) to the presence of a mantle plume. According to these authors, formation of dykes records an oblique collision of Fennoscandia with Sarmatia that started at c. 1.83-1.81 Ga and continued for the next c. 100 M.y. causing rotation of Sarmatia and extension of the crust that was accompanied by formation of transcrustal faults that served as channels for melt migration. A prolonged process of rotation and extension may explain the long duration of AMCG magmatism in the Ukrainian shield, whereas the relatively low heat input (compared with models for the generation of continental flood basalts), associated with this process accounts for the low melt production rate.

A model that involves melting of the depleted mantle in Andean-type arc systems to produce long-lived AMCG magmatism was discussed recently by Bybee et al. (2014a,b). However, there is no evidence of the Andean-type arc tectonic settings in the Ukrainian shield at the time of formation of the AMCG complexes. All available geological and geochemical data indicate a within-plate tectonic setting.

6.3. Hf isotopes support a mixed source of the parental melts for the Ukrainian AMCG complexes

A number of publications focus on Hf isotopes in zircons from rocks of AMCG complexes worldwide, and the data are mostly interpreted in term of a mixed crustal-mantle Hf isotope signature (Fig. 11). The same can be said for the Ukrainian AMCG complexes, although the isotope ratios appear to be dominated by the crustal end members. The average

hafnium isotope composition in zircons from the KPC basic rocks is close to the CHUR value at 1760 Ma: εHf varies from +0.4 to -3.5 (Table 5), and that from zircons in the silicic rocks is -1.2 (Fig. 8). In contrast, zircons from similarly aged high-Ni tholeiites in the North-Western region of the Ukrainian shield have more radiogenic Hf isotope compositions (εHf = +1.6 to +5.5) and appear to have been derived from a moderately depleted mantle source.

It has been concluded previously that the KPC parental melts might have inherited their Nd and Sr isotopic characteristics from the widely distributed lower crust generated in the 2.0-1.97 Ga Osnitsk-Mikashevychi orogeny (Shumlyanskyy et al., 2006). However, in order to explain the εNd_{1760} values over +0.5 these authors had to assume a limited input from mantle-derived tholeiitic melts (Fig. 8B). New Hf isotope data are in good agreement with this model. The εHf_{1990} in zircons from the Osnitsk-Mikashevychi igneous belt (granites and rhyolite) varies from -0.7 to +3.1 (Shumlyanskyy, 2014), with two outliers down to -4.8. If these values represent Hf isotope compositions of the Osnitsk-Mikashevychi rocks at the time of their formation, and taking into account an average $^{176}Lu/^{177}Hf = 0.012$ in these rocks (calculated from the measured whole rock Lu and Hf abundances), then the Hf isotope composition in the KPC zircons can be explained by the re-melting of the Osnitsk-Mikashevychi rocks at 1800-1750 Ma, with only minor input of juvenile Hf from mantle-derived high-Ni tholeiitic melts. Zircons from mafic pegmatites in high-Ni tholeiitic dolerites with their mantle-like Hf isotope ratios (see above) indicate that tholeiitic melts represent a suitable source of juvenile Hf (as well as of Sr and Nd) that was involved in petrogenesis of the KPC basic rocks. However, if a $^{176}Lu/^{177}Hf = 0.021$ value typical for a mafic crustal source (Kemp et al., 2006) is considered, then input of mantle Hf is not required. The metamorphic rocks of the Teteriv Series and granitoids of the Zhytomyr Complex (c. 2.2-2.05 Ga), which are also widely distributed in the North-Western region of the Ukrainian shield, may represent an alternative source of the Korosten melts (Fig. 8B).

Zircons from rocks of the KNPC tend to have lower εHf_T values varying from -2.4 to -3.5 that probably indicate older crustal material in their source or smaller input of juvenile material, compared to the KPC. Hf isotope data for the possible source rocks of the KNPC are not available, but Nd isotope data are summarised in Fig. 8B. The (Nd) model ages of the country rocks to the KNPC are slightly older than those for the KPC, and so are the (Hf) model ages for the KNPC zircons compared with those from the KPC (Fig. 8C). This highlights how the isotope ratios of the two complexes reflect those in the country rocks, providing striking evidence that the two complexes are largely derived from crustal source rocks heated, in the preferred model, by the emplacement of mafic magmas. Similar links between the isotope composition of Mid-Proterozoic anorthosites in the north-western Grenville Province of Ontario and the isotope composition of the ambient crust was explained by contamination of the mantle-derived basic melts during their ascent through the crust by two isotopically distinct lower crustal rock types (Prevec, 2004).

6.4. Model of formation of the Ukrainian AMCG complexes

Our model of formation of the Ukrainian AMCG complexes is based on the following observations: (1) mixed crustal-mantle isotope signature of all rocks that constitute both KPC and KNPC; (2) close links of the AMCG complexes with mantle-derived tholeiitic melts in space and time; (3) long duration of the AMCG magmatism at relatively low average melt production rates.

Evidence in favor of the mixed mantle-lower-crustal origin of the initial ferromonzodioritic melts includes: (1) the prominent Nb-Ta negative anomaly in the ferromonzodiorites, that is absent or greatly reduced in the coeval tholeiitic melts; (2) Hf and Nd isotope compositions of ferromonzodiorites conform to the model of re-melting of the

ambient crust but with some input of juvenile mantle-derived material; (3) the ferromonzodiorites have rather steep REE patterns [$(La/Yb)_N$ = 6.1-10.5] that may imply the presence of residual garnet in their source. Such source rocks can be represented by lower-crustal eclogite. In contrast, tholeiites have less fractionated REE [$(La/Yb)_N$ = 2.4-4.0] consistent with melt generation in the absence of garnet.

Melting of the mafic lower crust to produce ferromonzodioritic melts is thought to occur at 10-13 kbar (Longhi et al., 1999; Longhi, 2005), which corresponds to a depth of c. 40 km, and such depths are consistent with either a thickened crust, which is unlikely given the wide distribution of the mafic dykes or, alternatively, the lower crust was delaminated and displaced down into the mantle (cf. the crustal tongue melting model of Duchesne et al., 1999). As shown by Bogdanova et al. (2004), the crust beneath the KPC is marked by an elevated Moho (beneath the KPC the Moho discontinuity occurs at a depth of 38-39 km, whereas in the surrounding areas it is located at depths between 42 and 52 km), and in comparison with the ambient areas (Fig. 12), the crust is less dense and less magnetic. Thus, the underlying mantle lithosphere and part of the lower crust beneath AMCG plutonic complexes may have been lost by delamination and sunk into the mantle due to either "continuing movements and disturbances… during post-collisional tectonic events" (Bogdanova et al., 2004) or as a result of emplacement and ponding of mantle-derived tholeiitic melts which become eclogitized.

A model of formation of the AMCG complexes based on delamination of the lithosphere in a late- to post-orogenic tectonic setting has been proposed by many researchers (see Lee et al., 2014; Teng and Santosh, 2015, and references therein). This model envisages a replacement of the removed lithosphere by uprising asthenospheric mantle, and the generation of mafic magma is response to decompression, as a possible source of the AMCG suite (McLelland et al., 2010).

The close temporal and spatial links of the AMCG complexes and mantle-derived magmatism over relatively large areas can hardly be considered as a coincidence. Irrespective of their origin and the role of post-collisional rotation, these melts indicate the presence of a significant thermal anomaly that caused fusion of the mantle material. The increased heat flow and emplacement of the hot mantle melts heated up the crust, and tectonic disturbance caused by collision and the thermal erosion resulted in delamination of the lower crust and its sinking into the heated mantle (Fig. 12). The subsequent partial (c. 30 %, see Vander Auwera et al., 2011) melting of the mafic lower-crustal material and some interaction with mantle-derived tholeiitic melts resulted in formation of ferromonzodioritic melts that were initial melts for the basic rocks of the Ukrainian AMCG complexes. The progressive evolution of ferromonzodioritic melts included a stage of crystal fractionation and contamination of their derivatives by products of abundant melting of the middle crust. These resulting silicic melts gave rise to the whole spectrum of rapakivi granites and low-volume melts from which late-stage granite varieties were formed.

Arguing against the extensive lower-crustal melting, Bybee et al. (2014b, p. 383) noted that "the only reasonable mechanism to induce the required volume of melting would be upwelling mantle", which must be accompanied by "equally, if not more voluminous, coeval mafic melts (formed by decompression melting of the upwelling mantle) together with the anorthosites – a feature which is simply not observed around Proterozoic anorthosite massifs". However, as was shown above this does not appear to be true in the case of the Ukrainian shield, where voluminous products of the mantle melting are present.

7. Conclusions

This paper reviews existing geochronology and geochemistry data from the two AMCG complexes of the Ukraine shield, the Korosten plutonic complex (KPC) and the Korsun-Novomyrhorod plutonic complex (KNPC), and provides additional targeted U-Pb dating which leads to the following conclusions:

1. The whole assemblage of basic and silicic rocks in the northern part of the KPC was initially formed between c. 1800 and 1780 Ma. Magmatic activity temporarily ceased from c. 1780 Ma, to restart vigorously again at c. 1770 Ma. The majority of the KPC rocks that crop out at the surface formed between c. 1768 and 1755 Ma. The latest stages of the KPC evolution (1752-1743 Ma) are expressed by the formation of the minor intrusions of late subalkaline granites, veins of Li-F microcline-albite granites, and sill-like ferromonzodiorite intrusion.

2. In contrast to the KPC, most of the KNPC complex basic and silicic rocks emplaced simultaneously between c. 1757 and 1750 Ma, and the latest phases of the complex are represented by monzonites and syenites that were formed between 1748 and 1744 Ma. The emplacement of the KNPC slightly postdates the main intrusive phase of the KPC, whereas the majority of silicic and basic rocks intruded within a similar time interval of 10 M.y.

3. The KPC and KNPC were formed 150-200 M.y. after the last orogenic event. Geological and geochemical data indicate a within-plate tectonic setting of the AMCG magmatism in the Ukrainian shield.

4. The Hf isotope composition of zircons and Nd whole-rock isotope composition indicate a predominantly crustal source of the parental magma with some input of juvenile Hf and Nd from coeval mantle-derived tholeiite melts.

5. The preferred model of formation of the Ukrainian AMCG complexes envisages delamination of the mafic lower crust into the mantle, either in response to post-collisional tectonic disturbance or as a result of the emplacement of large volumes of hot mantle-derived

melts into the lower crust. These processes resulted in partial melting of mafic lower-crustal material, its mixing with the mantle-derived melts and formation of ferromonzodioritic melts. Further fractional crystallization of the ferromonzodioritic melts produced the spectrum of basic rocks that belong to the AMCG complexes. The emplacement of the ferromonzodioritic and tholeiitic melts into the middle crust and their partial crystallization caused profound melting of the ambient crust and formation of the whole spectrum of granitic rocks present in the complexes.

Acknowledgments

This research gained financial support granted by the Royal Society, UK (2006/R4 IJP), and the Swedish Institute, Sweden. We are indebted to O. Shestopalova who kindly provided zircons separated from a xenolith hosted by an anorthosite. Prof. Jean-Clair Duchesne is appreciated for his valuable discussion and suggestions. The paper has benefitted from constructive comments from Lewis D. Ashwal, Tom Andersen, and an anonymous reviewer. This paper is NORDSIM contribution number 484, and publication no. 62 of the Large Igneous Provinces – Supercontinent Reconstruction – Resource Exploration Project (CAMIRO Project 08E03, and NSERC CRDPJ 419503-11) (www.supercontinent.org, www.camiro.org/exploration/ongoing-projects), and a contribution to IGCP 648.

References

Alviola, R., Johanson, B.S., Rämö, O.T., Vaasjoki, M., 1999. The Proterozoic Ahvenisto rapakivi granite – massif-type anorthosite complex, southeastern Finland; petrography and U-Pb geochronology. Precambrian Res. 95, 89-107.

Amelin, Yu., Li, C., Naldrett, A.J., 1999. Geochronology of the Voisey's Bay intrusion, Labrador, Canada, by precise U-Pb dating of coexisting baddeleyite, zircon, and apatite. Lithos 47, 33-51.

Amelin, Yu.V., Heaman, L.M., Verchogliad, V.M., Skobelev, V.M., 1994. Geochronological constraints on the emplacement history of an anorthosite-rapakivi granite suite: U-Pb zircon and baddeleyite study of the Korosten complex, Ukraine. Contrib. Mineral. Petrol. 116, 411-419.

Amelin, Yu.V., Larin, A.M., Tucker, R.D., 1997. Chronology of multiphase emplacement of the Salmi rapakivi granite – anorthosite complex, Baltic shield: implications for magmatic evolution. Contrib. Mineral. Petrol. 127, 353-368.

Ashwal, L.D., 1993. Anorthosites. Springer-Verlag, Berlin, Germany. – 422 p.

Ashwal, L.D., Wooden, J.L., Emslie, R.F., 1986. Sr, Nd, and Pb isotopes in Proterozoic intrusives astride the Grenville Front in Labrador: Implications for crustal contamination and basement mapping. Geochim. Cosmochim. Acta 50, 2571-2585.

Bickford, M.E., McLelland, J.M., Mueller, P.A., Kamenov, G.D., Neadle, M., 2010. Hafnium isotopic compositions of zircon from Adirondack AMCG suites: implications for the petrogenesis of anorthosites, gabbros, and granitic members of the suites. Can. Mineral. 48, 751-761.

Bogdanova, S., Gorbatschev, R., Skridlaite, G., Soesoo, A., Taran, L., Kurlovich, D., 2015. Trans-Baltic Palaeoproterozoic correlations towards the reconstruction of supercontinent Columbia/Nuna. Precambrian Res. 259, 5-33.

Bogdanova, S.V., Gintov, O.B., Kurlovich, D., Lubnina, N.V., Nilsson, M., Orlyuk, M.I., Pashkevich, I.K., Shumlyanskyy, L.V., Starostenko, V.I., 2013. Late Palaeoproterozoic mafic dyking in the Ukrainian Shield (Volgo-Sarmatia) caused by rotations during the assembly of supercontinent Columbia. Lithos 174, 196–216.

Bogdanova, S.V., Pashkevich, I.K., Buryanov, V.B., Makarenko, I.A., Orlyuk, M.I., Skobelev, V.M., Starostenko, V.I., Legostaeva, O.V., 2004. The 1.80-1.74 Ga gabbro-anorthosite-rapakivi Korosten Pluton in the NW Ukrainian Shield: a 3-D geophysical reconstruction of deep structure. Tectonophysics 381, 5-27.

Bolle, O., Demaiffe, D., Duchesne, J.-C., 2003. Petrogenesis of jotunitic and acidic members of an AMC suite (Rogaland anorthosite province, SW Norway): a Sr and Nd isotopic assessment. Precambrian Res. 124, 185-214.

Bouvier, A., Vervoort, J. D., Patchett, P. J., 2008. The Lu–Hf and Sm–Nd isotopic composition of CHUR: constraints from unequilibrated chondrites and implication for the bulk composition of terrestrial planets. Earth and Planetary Science Letters, 273, 48–57.

Bybee, G.M., Ashwal, L.D., Shirey, S.B., Horan, M., Mock, T., Andersen, T.B., 2014a. Pyroxene megacrysts in Proterozoic anorthosites: implications for tectonic setting, magma source and magmatic processes at the Moho. Earth Planet. Sci. Lett. 389, 74–85.

Bybee, G.M., Ashwal, L.D., Shirey, S.B., Horan, M., Mock, T., Andersen, T.B., 2014b. Debating the petrogenesis of Proterozoic anorthosites – Reply to comments by Vander Auwera et al. on "Pyroxene megacrysts in Proterozoic anorthosites: implications for tectonic setting, magma source and magmatic processes at the Moho". Earth Planet. Sci. Lett. 401, 381-383.

Chauvel, C., Blichert-Toft, J., 2001. A hafnium isotope and trace element perspective on melting of depleted mantle. Earth Planet. Sci. Lett. 190, 137–151.

Chemale, F., Philipp, R.P., Dussin, I.A., Formoso, M.L.L., Kawashita, K., Berttotti, A.L., 2011. Lu–Hf and U–Pb age determination of Capivarita Anorthosite in the Dom Feliciano Belt, Brazil. Precambrian Res. 186, 117–126.

Chernyshov, N.M., Bayanova, T.B., Albekov, A.Yu., Levkovich, N.V., 2001. New data on age of the gabbroic dolerite intrusions of the continental flood basalt formation of the

Khoper block of the Voronezh crystalline massif (Central Russia). Proceed. Acad. Sci. USSR 380, 661–664. (In Russian).

Condie, K.C., 2005. High field strength element ratios in Archean basalts: a window to evolving sources of mantle plumes? Lithos 79, 491–504.

Dovbush, T.I., Stepanyuk, L.M., Shestopalova, E.E., 2009. Crystallogenesis and age of zircon in gabbroic rocks of the Korsun-Novomyrhorod pluton, Ukrainian shield. Geochem. Ore Formation 27, 20-23. (In Russian).

Duchesne, J. C., Wilmart, E., 1997. Igneous charnockites and related rocks from the Bjerkreim-Sokndal layered intrusion (Southwest Norway): a jotunite (hypersthene monzodiorite)-derived A-type granitoid suite. J. Petrol. 38, 337-369.

Duchesne, J.C., Liégeois, J.P., Vander Auwera, J., Longhi, J., 1999. The crustal tongue melting model and the origin of massive anorthosites. Terra Nova 11, 100–105.

Duchesne, J.-C., Martin, H., Bagiński, B., Wiszniewska, J., Vander Auwera, J., 2010. The origin of ferroan-potassic A-type granitoids: the case of the hornblende–biotite granite suite of the Mesoproterozoic Mazury complex, northeastern Poland. Can. Mineral. 48, 947-968.

Duchesne, J.C., Roelandts, I., Demaiffe, D., Weis, D., 1985. Petrogenesis of monzonoritic dykes in the Egersund-Ogna anorthosite (Rogaland, S.W. Norway): trace elements and isotopic (Sr, Pb) constraints. Contrib. Mineral. Petrol. 90, 214-225.

Duchesne, J.C., Shumlyanskyy, L., Charlier, B., 2006. The Fedorivka layered intrusion (Korosten Pluton, Ukraine): an example of highly differentiated ferrobasaltic evolution. Lithos 89, 353-376.

Emslie, R.F., 1991. Granitoids of rapakivi granite-anorthosite and related associations. Precambrian Res. 51, 173-192.

Emslie, R.F., Hamilton, M.A., Thériault, R.J., 1994. Petrogenesis of a Mid-Proterozoic anorthositemangerite-charnockite-granite (AMCG) complex: isotopic and chemical evidence from the Nain plutonic suite. J. Geol. 102, 539-558.

Emslie, R.F., Hegner, E., 1993. Reconnaissance isotopic geochemistry of anorthosite-mangerite-charnockite-granite (AMCG) complexes, Grenville Province, Canada. Chem. Geol. 106, 279-298.

Ernst, R.E., 2014. Large Igneous Provinces. Cambridge University Press, 653 p.

Esipchuk, K.E., Sheremet, E.M., Zinchenko, O.V., Bobrov, A.B., Borko, V.N., Bukharev, S.V., Vesilchenko, V.V., Verkhogliad, V.M., Golub, E.N., Demyanenko, V.V., Zhebrovskaya, E.I., Orsa, V.I., Panov, B.S., Razdorozhny, V.F., Sveshnikov, K.I., Skobelev, V.M., Shcherbak, D.N., 1990. Petrology, geochemistry and metallogeny of the intrusive granitoids of the Ukrainian shield. Kyiv, Naukova Dumka, 236 p. (In Russian).

Fisher, C.M., Hanchar, J.M., Samson, S.D., Dhuime, B., Blichert-Toft, J., Vervoort, J.D., Lam, R., 2011. Synthetic zircon doped with hafnium and rare earth elements: A reference material for in situ hafnium isotope analysis. Chem. Geol. 286, 32–47.

Frost, C.D., Frost, B.R., 1997. Reduced rapakivi-type granites: the tholeiite connection. Geology 25, 647–650.

Gleißner, P., Drüppel, K., Romer, R.L., 2011. The role of crustal contamination in massif-type anorthosites, new evidence from Sr-Nd-Pb isotopic composition of the Kunene Intrusive Complex, NW Namibia. Precambrian Res. 185, 18-36.

Heinonen, A.P., Andersen, T., Rämö, O.T., 2010. Re-evaluation of rapakivi petrogenesis: source constraints from the Hf isotope composition of zircon in the rapakivi granites and associated mafic rocks of southern Finland. J. Petrol. 51, 1687-1709.

Heinonen, A.P., Fraga, L.M., Rämö, O.T., Dall'Agnol, R., Mänttäri, I., Andersen, T., 2012. Petrogenesis of the igneous Mucajaí AMG complex, northern Amazonian craton –

geochemical, U–Pb geochronological, and Nd–Hf–O isotopic constraints. Lithos 151, 17–34.

Higgins, M.D., van Breemen, O., 1996. Three generations of anorthosite-mangerite-charnockite-granite (AMCG) magmatism, contact metamorphism and tectonism in the Saguenay – Lac-Saint-Jean region of the Grenville province, Canada. Precambrian Res. 79, 327-346.

Kemp, A. I. S., Foster, G. L., Scherstén, A., Whitehouse, M. J., Darling, J., Storey, C., 2009. Concurrent Pb–Hf isotope analysis of zircon by laser ablation multi-collector ICP-MS, with implications for the crustal evolution of Greenland and the Himalayas. Chem. Geol. 261, 244–260.

Kemp, A.I.S., Hawkesworth, C.J., Paterson, B.A., Kinny, P.D., 2006. Episodic growth of the Gondwana supercontinent from hafnium and oxygen isotopes in zircon. Nature 439, 580–583.

Krogh, T.E., 1973. A low contamination method for hydrothermal decomposition of zircon and extraction of U and Pb for isotopic age determinations. Geochim. Cosmochim. Acta 37, 485–494.

Lee, Y., Cho, M., Cheong, W., Yi, K., 2014. A massif-type (~1.86 Ga) anorthosite complex in the Yeongnam Massif, Korea: late-orogenic emplacement associated with the mantle delamination in the North China Craton. Terra Nova 26, 408–416.

Longhi, J., 2005. A mantle or mafic crustal source for Proterozoic anorthosites? Lithos 83, 183–198.

Longhi, J., Vander Auwera, J., Fram, M.F., Duchesne, J.C., 1999. Some phase equilibrium constraints of the origin of Proterozoic (massif) anorthosites and related rocks. J. Petrol. 40, 339-362.

Lubnina, N.V., Bogdanova, S.V., Shumlyanskyy, L.V., 2009. The East European Craton in the Palaeoproterozoic: new paleomagnetic data on magmatic complexes in the Ukrainian Shield. Geofizika (Geophysics) 5, 56–64. (In Russian).

Ludwig, K.R., 2012. Isoplot 3.75. A Geochronological toolkit for Microsoft Excel. Berkeley Geochronology Center. Spec. Pub. 5, p. 75.

McLelland, J.M., Selleck, B.W., Hamilton, M.A., Bickford, M.E., 2010. Late- to post-tectonic setting of some major Proterozoic anorthosite-mangerite-charnockite-granite (AMCG) suites. Can. Mineral. 48, 729–750.

Mitrokhin, A.V., Bilan, E.V., 2014. Petrology of 'hybrid rocks' related to the Korosten anorthosite-rapakivi granite pluton of the Ukrainian shield. Mineral. J. (Ukraine) 36 (2), 102-118. (In Russian).

Mitrokhin, A.V., Bogdanova, S.V., Shumlyanskyy, L.V., 2008. Polybaric crystallization of anorthosite of the Korosten pluton, Ukrainian shield. Mineral. J. (Ukraine) 30 (2), 36-56. (In Russian).

Mitrokhin, O.V., 2001. The gabbro-anorthosite massifs of the Korosten pluton (Ukraine) and problems of parental magmas evolution. Abstract volume of the GEODE field workshop 8-12th July 2001 on ilmenite deposits in the Rogaland anorthosite province, S. Norway. NGU Report #2001.042., 86-90.

Morisset, C.-E., Scoates, J.S., Weis, D., Friedman, R.M., 2009. U-Pb and $^{40}Ar/^{39}Ar$ geochronology of the Saint-Urbain and Lac Allard (Havre-Saint-Pierre) anorthosites and their associated Fe-Ti oxide ores, Québec: evidence for emplacement and slow cooling during the collisional Ottowan orogeny in the Grenville Province. Precambrian Res. 174, 95-116.

Mytrokhn, O.V., Bogdanova, S.V., Shumlyanskyy, L.V., 2003. Anorthosite rocks of the Fedorivskyy suite (the Korosten pluton, the Ukrainian shield). Current problems in geology, Kyiv National University, 53-57.

Owens, B.E., Rockow, M.W., Dymek, R.F., 1993. Jotunites from the Grenville Province, Quebec: petrological characterization and implication for massif anorthosite petrogenesis. Lithos 30, 57-80.

Ponomarenko, O.M., Zayats, O.V., Bezvynnyj, V.P., Tsyba, M.M., Dovbush, T.I., 2011. Composition and isotope age of the Ruska Polyana rare-metal granites of the Ukrainian shield. Geochem. Ore Formation 30, 18-26. (In Ukrainian).

Prevec, S.A., 2004. Basement tracing using Mid-Proterozoic anorthosites straddling a palaeoterrane boundary, Ontario, Canada. Precambrian Res. 129, 169–184.

Rämö, O.T., Haapala, I., 1996. Rapakivi granite magmatism: a global review with emphasis on petrogenesis. In: Demaiffe D. (ed). Petrology and geochemistry of magmatic suites of rocks in the continental and oceanic crust. A volume dedicated to Prof. J. Michot, 177-200.

Rämö, O.T., Haapala, I., 2005. Rapakivi granites. In: Lehtinen, M., Nurmi, P.A., Rämö, O.T. (eds) Precambrian geology of Finland – key to the evolution of the Fennoscandian shield. Elsevier, Amsterdam, 533–562.

Robins, B., Tumyr, O., Tysseland, M., Garmann, L.B., 1997. The Bjerkreim-Sokndal Layered Intrusion, Rogaland, SW Norway: Evidence from marginal rocks for jotunite parent magma. Lithos 39, 121-133.

Schärer, U., Wilmart, E., Duchesne, J.C., 1996. The short duration and anorogenic character of anorthosite magmatism: U-Pb dating of the Rogaland complex, Norway. Earth Planet. Sci. Lett. 139, 335-350.

Schiellerup, H., Lambert, D.D., Presvik, T., Robins, B., McBride, J.S., Larsen, R.B., 2000. Re-Os isotopic evidence for a lower crustal origin of massif-type anorthosites. Nature 405, 781-784.

Scoates, J.S., Frost, C.D., 1996. A strontium and neodymium isotopic investigation of the Laramie anorthosites, Wyoming, USA: implications for magma chamber processes and the evolution of magma conduits in Proterozoic anorthosites. Geochim. Cosmochim. Acta 60, 95-107.

Segal, I., Halicz, L., Platzner, I. T., 2003. Accurate isotope ratio measurements of ytterbium by multicollector inductively coupled plasma mass spectrometry applying erbium and hafnium in an improved double external normalisation procedure. J. Anal. At. Spectrom. 18, 1217–1223.

Shcherbak, N.P., Artemenko, G.V., Bartnitsky, E.N., Verkhogliad, V.M., Komaristy, A.A., Lesnaya, I.M., Mitskevich, N.Yu., Ponomarenko, A.N., Skobelev, V.M., Shcherbak, D.N., 1989. Geochronological chart of the Precambrian of the Ukrainian shield. Kyiv, Naukova dumka, 144 p. (In Russian).

Shcherbak, N.P., Artemenko, G.V., Lesnaya, I.M., Ponomarenko, A.N., Shumlyanskyy, L.V., 2008. Geochronology of the early Precambrian of the Ukrainian shield. Proterozoic. Kyiv, Naukova dumka, 240 p. (In Russian).

Shcherbakov, I.B., 2005. Petrology of the Ukrainian shield. Lviv, 366 p. (In Russian).

Sheremet, Ye.M., Melnikov, V.S., Strekozov, S.N., Kozar, N.A., Voznyak, D.K., Kulchitskaya, A.A., Kryvdik, S.G., Borodynya, B.V., Volkova, T.P., Sedova, E.V., Omelchenko, A.A., Nikolayev, I.Yu., Nikolayev, Yu.I., Setaya, L.D., Agarkova, N.G., Grechanovskaya, Ye.Ye., Foschiy, N.V., Ekaterinenko, V.N., 2012. Azov rare-earth deposit of the Azov region of the Ukrainian shield. “Knowledge” publishing house, Donetsk, 374 p.

Shestopalova, E.E., Stepanyuk, L.M., Dovbush, T.I., Kovtun, A.V., 2014. On the age of white anorthosites of the Novomyrhorod massif of the Korsun-Novomyrhorod pluton, Ukrainian shield. Geophys. J. 36 (2), 150-160. (In Russian).

Shestopalova, O.T., Stepanyuk, L.M., Dovbush, T.I., 2010. U-Pb orthite age of rapakivi granite of the Korsun-Novomyrhorod pluton. Abstract volume of the International conference "Stratigraphy, geochronology and correlation of the Early Precambrian rock complexes of the basement of the East European platform", UkrDGRI, 246-249. (In Ukrainian).

Shestopalova, O.T., Stepanyuk, L.M., Dovbush, T.I., Syomka, V.O., Bondarenko, S.M., Prykhodko, E.S., 2013. The Palaeoproterozoic granitoid magmatism of the Ingul terrain of the Ukrainian shield. Granidoids: conditions of their formation and ore potential. Abstract vol. of the scientific conference, 27 May – 1 June, Kyiv, Ukraine, 152-153. (In Russian).

Shumlyanskyy, L, Mitrokhin, O., Billström, K., Ernst, R., Vishnevska, E., Tsymbal, S., Cuney, M., Soesoo, A., 2016b. The ca. 1.8 Ga mantle plume related magmatism of the central part of the Ukrainian shield. GFF 138, 86-101.

Shumlyanskyy, L., 2014. Geochemistry of the Osnitsk-Mikashevichy volcanoplutonic complex of the Ukrainian shield. Geochem. Int. 52, 912–924.

Shumlyanskyy, L., Billström, K., Hawkesworth, C., Elming, S.-Å., 2012. U-Pb age and Hf isotope compositions of zircons from the north-western region of the Ukrainian shield: mantle melting in response to post-collision extension. Terra Nova 24, 373-379.

Shumlyanskyy, L., Ellam, R.M., Mitrokhin, O., 2006. The origin of basic rocks of the Korosten AMCG complex, Ukrainian shield: implication of Nd and Sr isotope data. Lithos 90, 214-222.

Shumlyanskyy, L., Ernst R., Söderlund, U., Billström, K., Mitrokhin, O., Tsymbal, S., 2016a. New U-Pb ages for mafic dykes in the Northwestern region of the Ukrainian shield: coeval tholeiitic and jotunitic magmatism. GFF 138, 79-85.

Shumlyanskyy, L.V., Bogdanova, S.V., 2009. U-Pb age of zircons and geochemistry of rhyolites of the Ovruch depression, North-Western region of the Ukrainian shield. Mineral. J. (Ukraine) 31 (1), 40-49. (In Ukrainian).

Shumlyanskyy, L.V., Mazur, M.D., 2010. Age and composition of the jotunites of the Bilokorovychi dyke swarm. Geologist of Ukraine 1-2, 70-78. (In Ukrainian).

Shumlyanskyy, L.V., Zagnitko, V.M., 2011. Isotope age, geochemistry and mineralogy of pegmatites in anorthosites of the Volodarsk-Volynsky massif, Korosten plutonic complex. Mineral. J. (Ukraine) 33 (1), 15-29. (In Ukrainian).

Söderlund, U., Patchett, J. P., Vervoort, J. D., Isachsen, C. E., 2004. The ^{176}Lu decay constant determined by Lu–Hf and U–Pb isotope systematics of Precambrian mafic intrusions. Earth Planet. Sci. Lett. 219, 311–324.

Stacey, J.S., Kramers, J.D., 1975. Approximation of Terrestrial lead isotope evolution by a two-stage model. Earth Planet. Sci. Lett. 26, 207–221.

Steiger, R. H., Jäger, E., 1977. Subcommission on geochronology: convention of the use of decay constants in geo- and cosmo-chronology. Earth Planet. Sci. Lett. 36, 359–362.

Taylor, S. R., Campbell, I.H., McCulloch, M.T., McLennan, S.M., 1984. A lower crustal origin for massif-type anorthosites. Nature 311, 372-374.

Teng, X., Santosh, M., 2015. A long-lived magma chamber in the Paleoproterozoic North China Craton: Evidence from the Damiao gabbro-anorthosite suite. Precambrian Res. 256, 79–101.

Vaasjoki, M., Rämö, O.T., Sakko, M., 1991. New U-Pb ages from the Wiborg rapakivi area: constraints on the temporal evolution of the rapakivi granite-anorthosite-diabase dyke association of southeastern Finland. Precambrian Res. 51, 227-243.

Vander Auwera, J., Bolle, O., Bingen, B., Liégeois, J.-P., Bogaerts, M., Duchesne, J.C., De Waele, B., Longhi, J., 2011. Sveconorwegian massif-type anorthosites and related granitoids result from post-collisional melting of a continental arc root. Earth-Sci. Rev., 107, 375–397.

Vander Auwera, J., Longhi, J., Duchesne, J.C., 1998. A liquid line of descent of the jotunite (hypersthene monzodiorite) suite. J. Petrol. 39, 439-468.

Verkhogliad, V.M., 1995. Age stages of the Korosoten plutonic magmatism. Geochem. Ore formation 21, 34-47. (In Russian).

Vervoort, J.D., Patchett, P.J., Söderlund, U., Baker, M., 2004. The isotopic composition of Yb and the precise and accurate determination of Lu concentrations and Lu/Hf ratios by isotope dilution using MC-ICPMS. Geochemistry Geophysics Geosystems DOI 2004GC000721RR.

White, S. M., Crisp, J. A., Spera, F. J., 2006. Long-term volumetric eruption rates and magma budgets. Geochemistry, Geophysics, Geosystems, 7 (3), 1-20.

Whitehouse, M.J., Kamber, B.S., 2005. Assigning dates to thin gneissic veins in high-grade metamorphic terranes: a cautionary tale from Akilia, southwest Greenland. J. Petrol. 46, 291–318.

Wiedenbeck, M., Alle, P., Corfu, F., Griffin, W.L., Meier, M., Oberli, F., Von Quadt, A., Roddick, J.C., Spiegel, W., 1995. Three natural zircon standards for U-Th-Pb, Lu-Hf, trace element and REE analysis. Geostandards Newsletter 19, 1–23.

Wilson, J.R., Overgaard, G., 2005. Relationship between the Layered Series and the overlying evolved rocks in the Bjerkreim-Sokndal Intrusion, southern Norway. Lithos 83, 277– 298.

Wiszniewska, J., Claesson, S., Stein, H., Vander Auwera, J., Duchesne, J.-C., 2002. The north-eastern Polish anorthosite massif: petrological, geochemical and isotopic evidence for a crustal derivation. Terra Nova 14, 451-460.

Zhang, S.-H., Liu, S.-W., Zhao, Y., Yang, J.-H., Song, B., Liu, X.-M., 2007. The 1.75-1.68 Ga anorthosite-mangerite-alkali granitoid-rapakivi granite suite from the northern North China Craton: Magmatism related to a Paleoproterozoic orogen. Precambrian Res. 155, 287-312.

Figure captions

Figure 1. Sketch map of the Ukrainian shield. The North-Western Domain (I on the map) comprises two orogenic belts: (1) the Teteriv-Zhytomyr belt composed of the Teteriv Series amphibolite-facies metamorphic rocks (c. 2200-2100 Ma), and the Zhytomyr Complex granites (c. 2090-2040 Ma); and (2) the Osnitsk-Mikashevychi igneous belt (c. 2000 Ma). The Ingul Domain (III on the map) is predominantly made of c. 2060-2020 Ma granites and related rocks of the Novoukrainka and Kropivnytsky (formerly Kirovograd) Complexes. The amphibolite-facies metamorphosed supracrustals of the Ingul-Ingulets Series (c. 2300 Ma) are less abundant.

Figure 2. Sketch map of the Korosten plutonic complex (KPC) with locations of dated samples and ages in Ma (Table 1).

Figure 3. Sketch map of the Korsun-Novomyrhorod plutonic complex (KNPC) with locations of dated samples and ages in Ma (Table 1).

Figure 4. CL images of zircons from rocks of the Korosten plutonic complex.

Figure 5. U-Pb isotope diagrams for rocks of the Korosten plutonic complex.

Figure 6. CL images of zircons from rocks of the Korsun-Novomyrhorod plutonic complex.

Figure 7. U-Pb isotope diagrams for rocks of the Korsun-Novomyrhorod plutonic complex.

Figure 8. A: Hafnium isotope evolution diagram for zircons from rocks of the Korosten and Korsun-Novomyrhorod plutonic complexes. Hafnium isotope compositions in zircons from coeval tholeiite dykes and layered intrusions (Shumlyanskyy et al., 2012) are also shown.

B. Nd isotope ratios in rocks of the Korosoten and Korsun-Novomyrhorod plutonic complexes, and in mantle-derived tholeiites. The isotope composition of the most rocks in both complexes can be explained by the re-melting of the country rocks (Teteriv-Zhytomyr belt and Osnitsk-Mikashevychi igneous belt for the KPC and igneous rocks of the Ingul domain for the KNPC). However, some of the rocks have radiogenic Nd isotope composition (high εNd) that indicate input of mantle-derived melts. Thus the isotope data indicate mixed mantle-crustal source of the initial melts for the Ukrainian AMCG complexes.

Figure 9. Diagram showing the distribution of ages of rocks of the Korosten and Korsun-Novomyrhorod plutonic complexes. The ages of the Ukrainian shield mafic dykes are also shown.

Figure 10. Diagram showing mantle compositional components for ferromonzodioritic dykes and chilled margins of gabbroic intrusions of the Korosten plutonic complex and for Ni-bearing tholeiitic dykes and layered intrusions of the Ukrainian shield. Ferromonzodioritic dykes and chilled margins represent parental melts from which basic rocks of the KPC have crystallized that enables direct comparison with tholeiitic dykes. Korosten initial melts fall in the field of arc-related basalts and gravitate towards the upper continental crust indicating their non-plume origin. In contrast, tholeiitic dykes plot in the fields of oceanic plateau basalts and ocean island basalts close to the primitive mantle and enriched mantle markers that reveal their plume-related origin. Abbreviations and fields are according to Condie (2005), and references therein: UC, upper continental crust; PM, primitive mantle; DM, shallow depleted mantle; HIMU, high-μ (U/Pb) source; EM1 and EM2, enriched mantle sources; ARC, arc-related basalts; NMORB, normal ocean ridge basalt; OIB, oceanic island basalt; DEP, deep depleted mantle; EN, enriched component; REC, recycled component.

Figure 11. Variations in the initial εHf values in zircons from rocks of the AMCG complexes worldwide. The data indicate variability of the sources of the initial melts for the AMCG complexes consistent with a mixed crustal-mantle Hf isotope signature. The origins of most of the rocks, even with the most depleted Hf isotope signature, can be generally explained by the melting of (or the contamination by) the juvenile continental crust.

Figure 12. A cross-section model illustrating the proposed relationships between the key magmatic phases in the Korosten AMCG complex. The figure is based on the initial geological interpretation of the deep structure of the Korosten complex (Bogdanova et al., 2004, Fig. 11), supplemented by the new (herein) and published geochronological results.

Fig. 2

29° E
51° N
33° E
49° N
37° E
47° N

I
II
III
IV
V
VI

Fig. 3

Paleoproterozoic

- Granitoids and amphibolite-facies metamorphosed supracrustal rocks (2300-2000 Ma)
- Granitoids and related rocks of the Novoukrainka massif (c.2040 Ma)
- Igneous rocks of the Osnitsk-Mikashevychi Igneous Belt and synchronous intrusions (2000-1970 Ma)
- Sediments of the Bilokorovychi basin (1950-1800 Ma)
- Sedimentary and volcanogenic rocks of the Ovruch and Vilcha basins (<1760 Ma)

Korosten and Korsun-Novomyrgorod AMCG complexes:

- Granitoids
- Basic rocks

Domains:

I - North-Western
II - Ros-Tikych
III - Ingul
IV - Dniester-Bug
V - Middle Dnieper
VI - Azov

Archaean

- Predominantly Eo- and Paleoarchaean rock complexes
- Predominantly Mesoarchaean rock complexes
- Mesoarchaean greenstone belts
- Neoarchaean to Palaeoproterozoic BIFs
- Neoarchaean granitoids

0 200 km

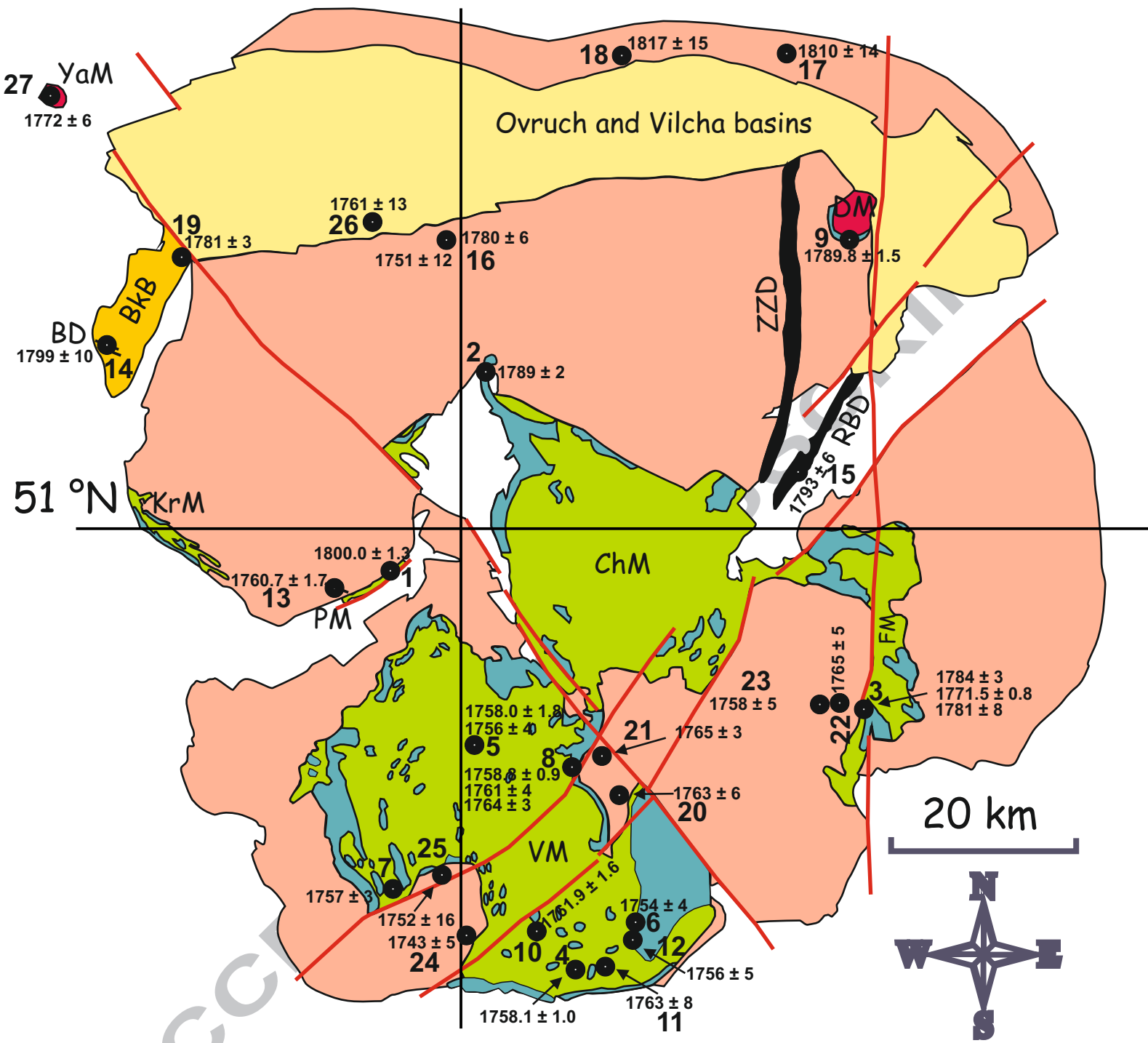

- Sedimentary rocks of the Bilokorovychi basin (BkB)
- Metavolcanites and sedimentary rocks of the Ovrucha nd Vilcha basins
- Anorthosites and related rocks (VM - Volynsky, ChM - Chopovychi, FM - Fedorivka, KrM - Kryvotin massif, and PM - Pugachivka massifs)
- Gabbro, melagabbro
- Gabbro-syenites and syenites (DM - Davydky, YaM - Yastrebetsky massifs)
- Dykes (ZZD - Zvizdal-Zalissya, RBD - Rudnya-Bazarska, BD - Bilokorovychi)
- Rapakivi granites and related rocks
- Host rocks
- Major faults

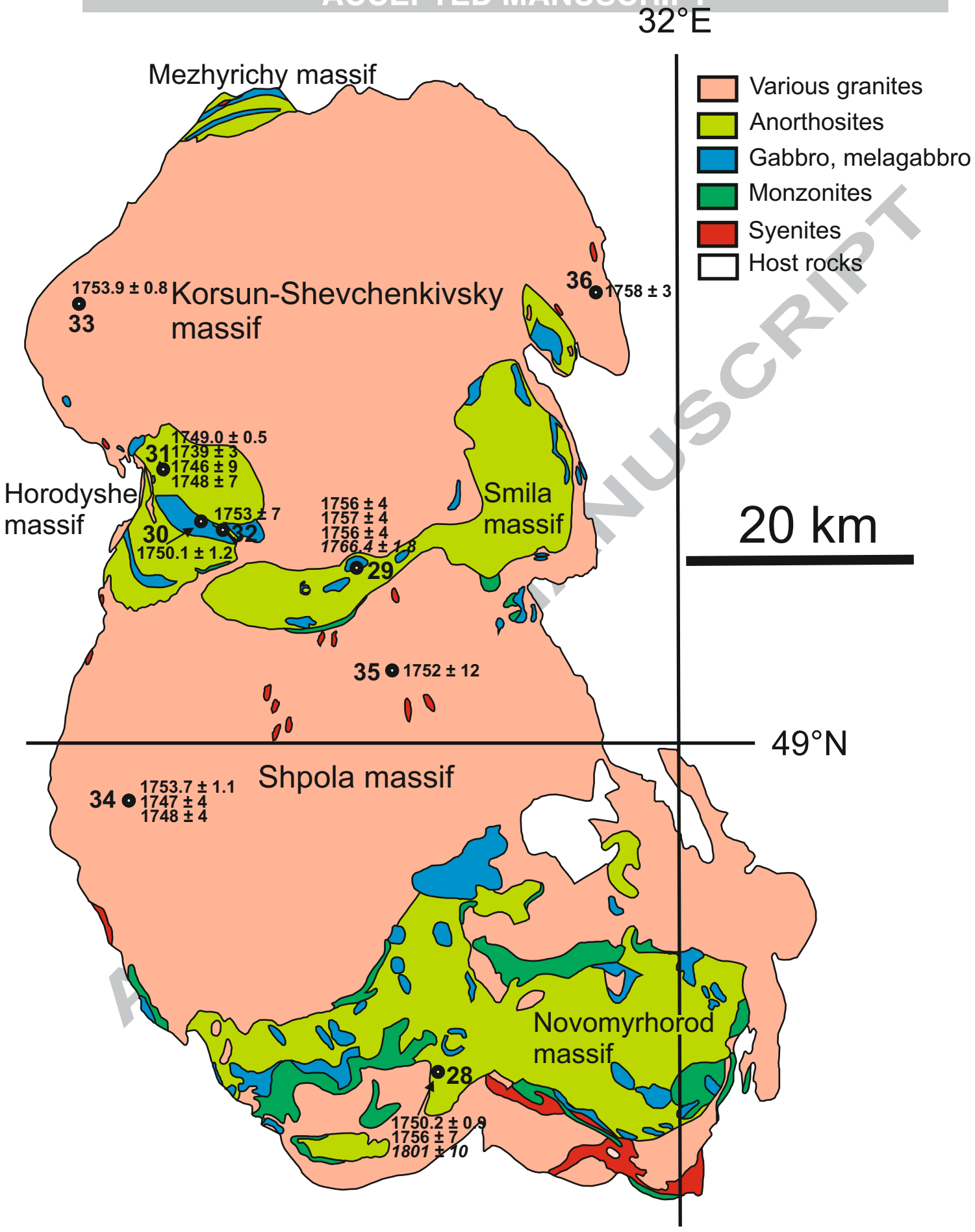

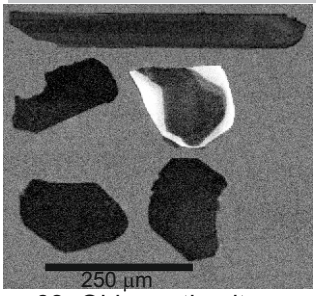

68. Old anorthosite

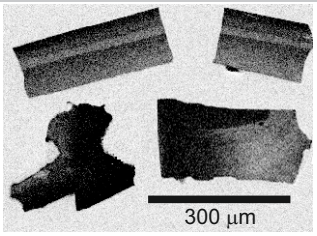

Parom. Pegmatite in anorthosite

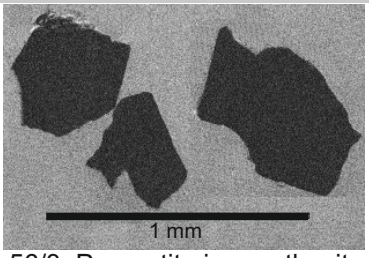

56/3. Pegmatite in anorthosite

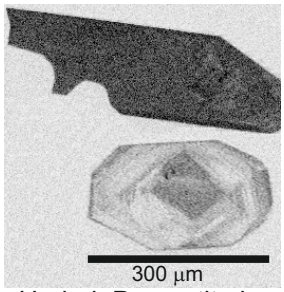

Horbul. Pegmatite in anorthosite

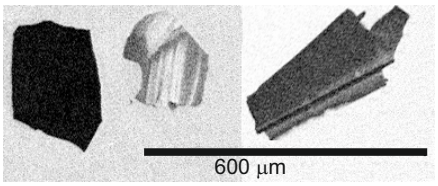

599. Olivine gabbro

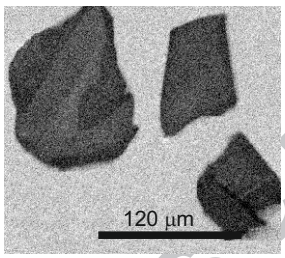

03-D24. Gabbro

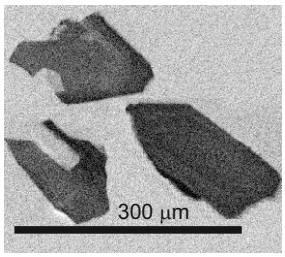

03-D18. Gabbro

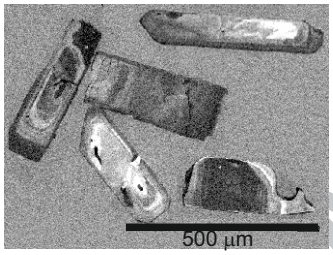

71-1M. Monzogabbro

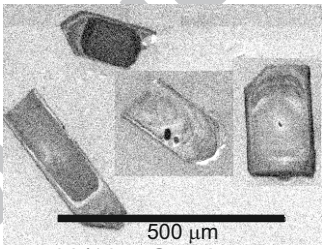

503/105. Granite

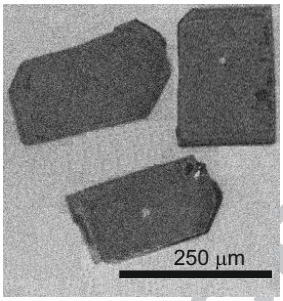

75/146. Granite

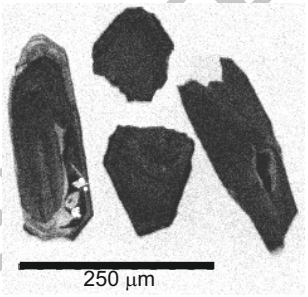

06-BG48. Granite

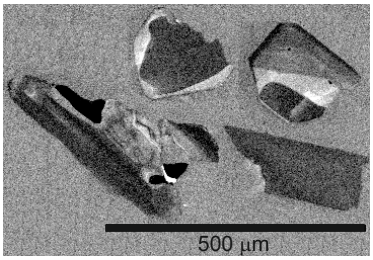

53-7. Granite

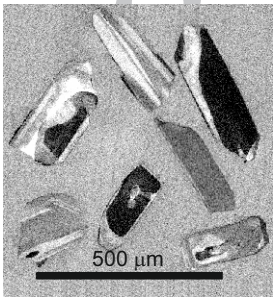

95005. Granite

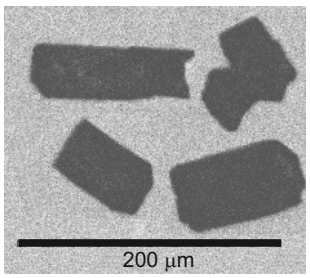

03-D1. Rare metal granite

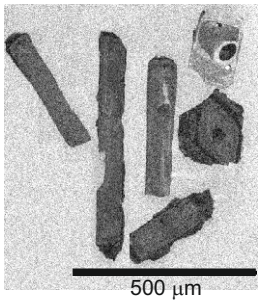

71-9. Syenite

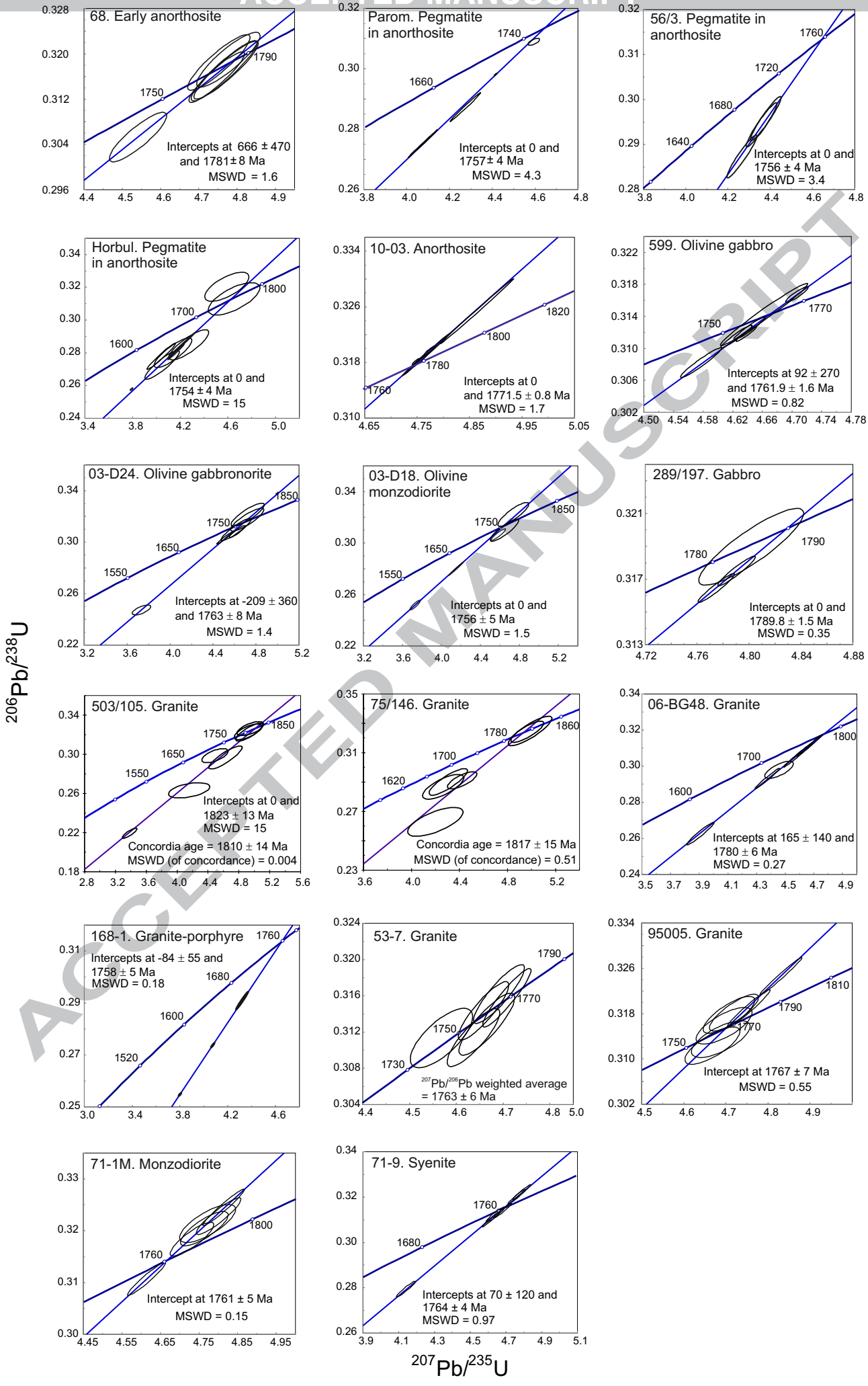

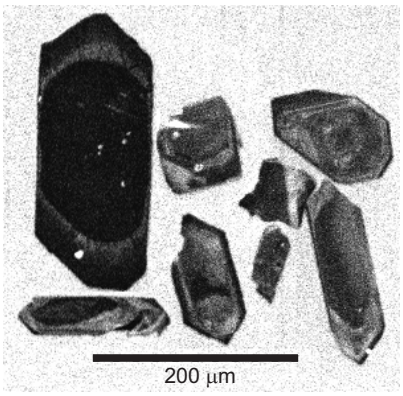

06-BG4. Quartz monzonite

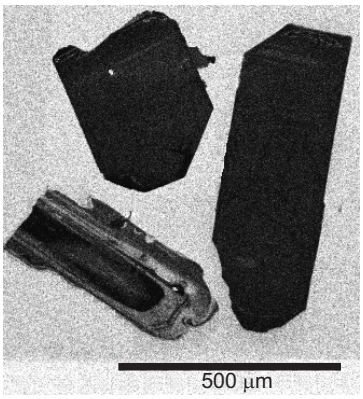

06-BG5. Quartz syenite

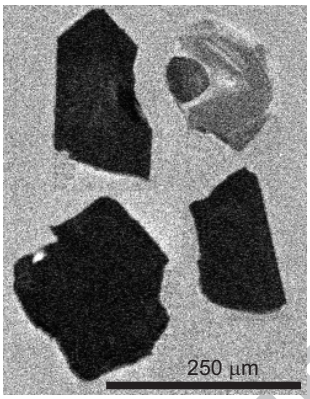

2006. Gabbro

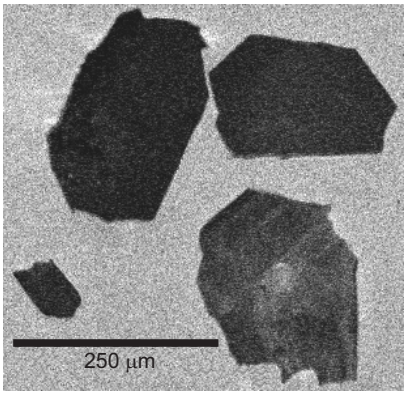

2008. Gabbro

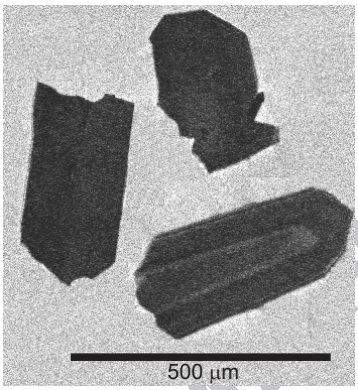

2004. Anorthosite

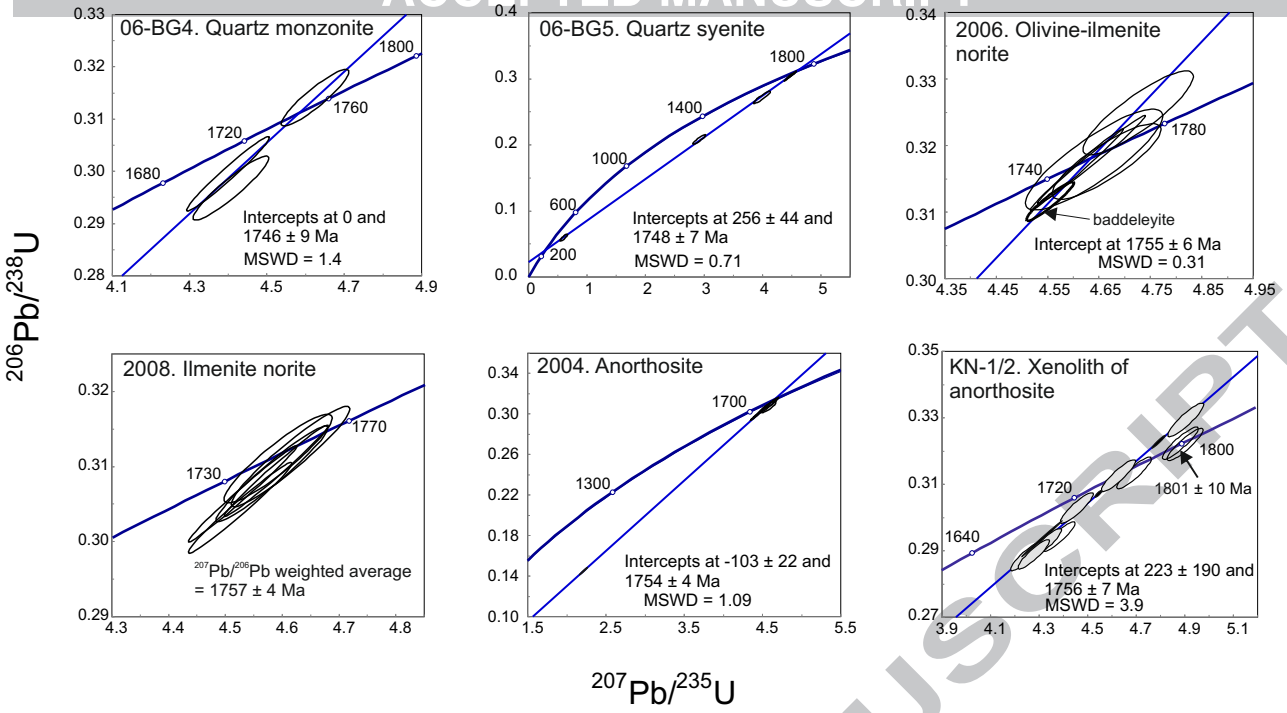

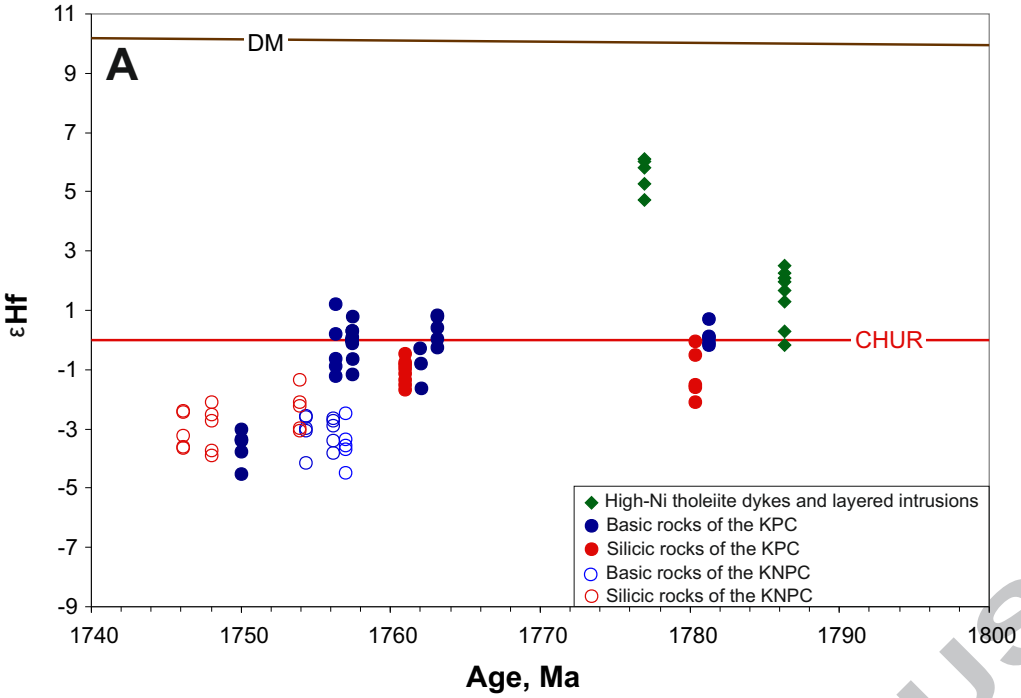

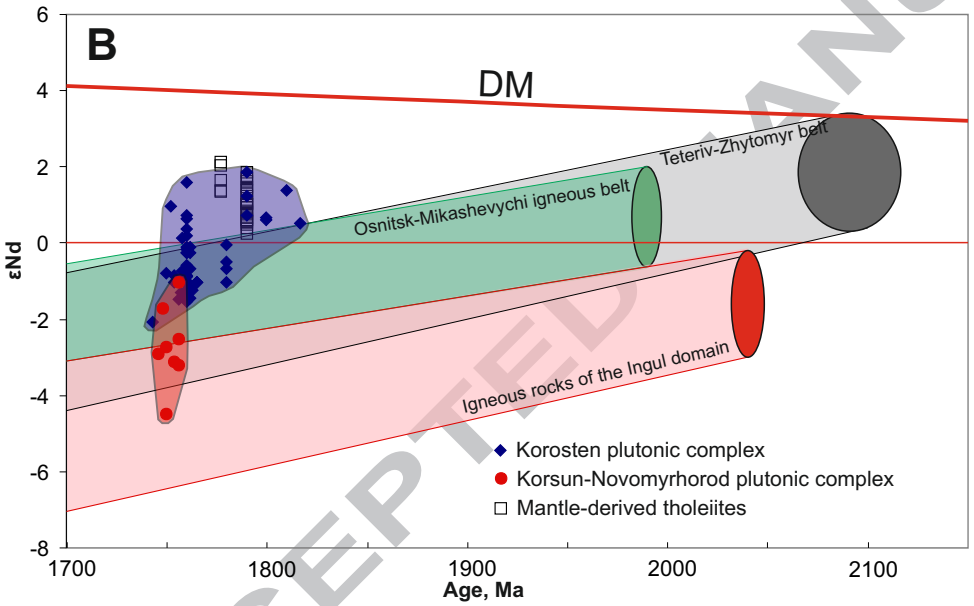

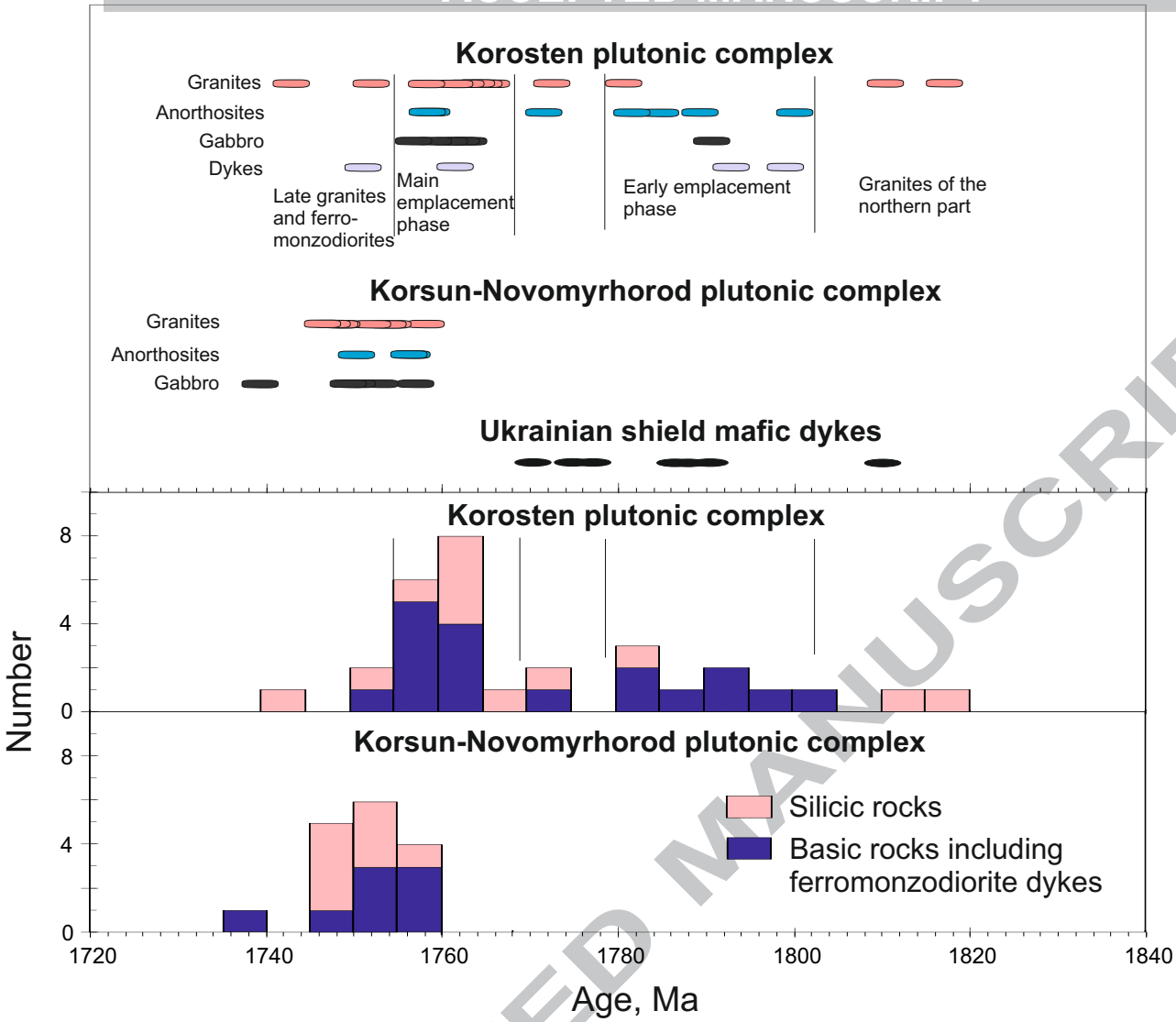

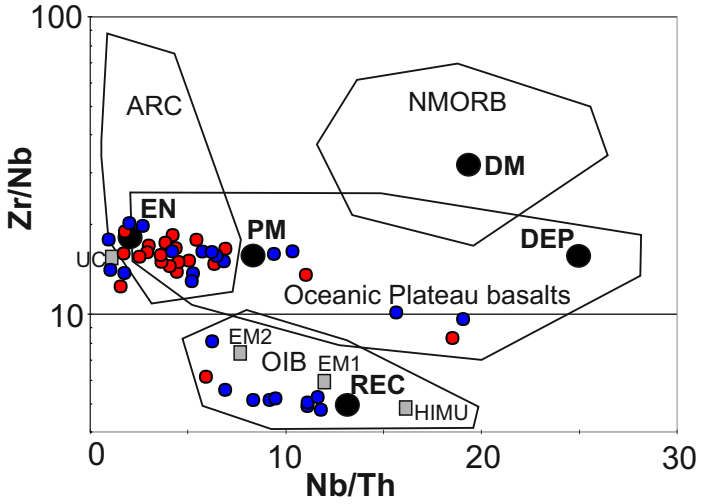

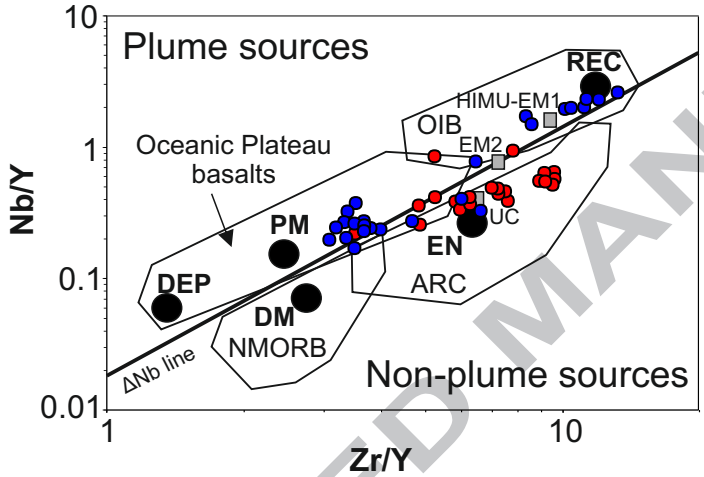

Ni-bearing tholeiitic dykes and layered intrusions of the Ukrainian shield

Ferromonzodioritic dykes and chilled margins of the Korosten plutonic complex

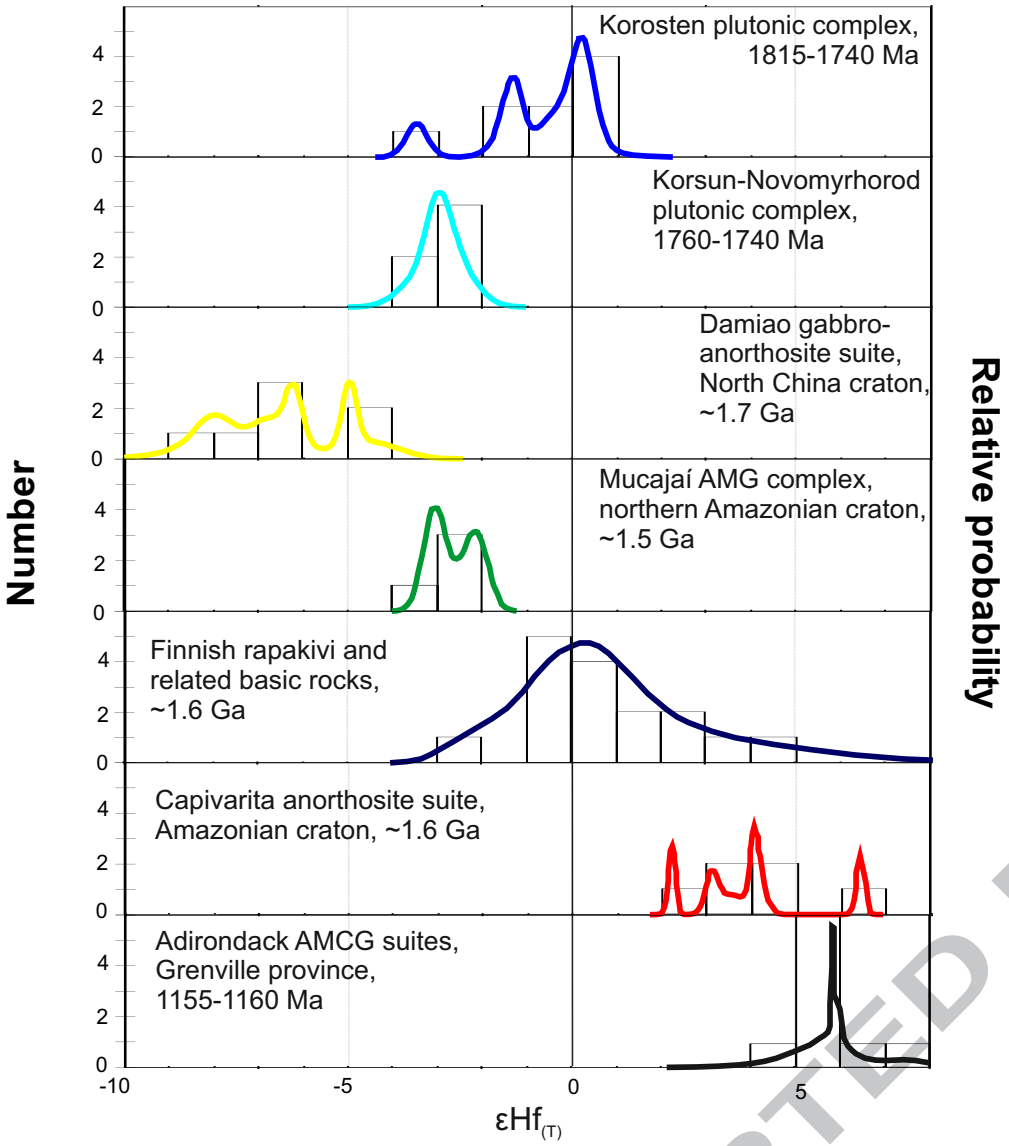

A lower-crustal mafic material is considered as a major source of the ferromonzodioritic parental melt, with some input of juvenile material from the mantled-derived tholeiitic melts. Silicic rocks were produced due to partial melting of the lower- and mid-crustal material

A remobilisation of Archaean continental crust into the mantle-derived melt (Zhang et al., 2007; Teng and Santosh, 2015)

A predominantly crustal source component in the parental magmas (Heinonen et al., 2012)

An involvement of a homogeneous Palaeoproterozoic crustal source for the felsic rocks, and a depleted, MORB-like mantle component for the basic rocks (Heinonen et al., 2010)

A juvenile source with some degree of Palaeoproterozoic crustal contamination (Chemale et al., 2011)

A felsic melt was generated due to partial melting of the older crust or mantle lithosphere, or both, whereas basic rocks crystallized from basaltic melts originated from enriched mantle lithosphere. The initial melts were produced from ~ 1350 Ma old crust and sub-arc mantle that were relatively homogeneous in terms of Hf isotopic composition and Lu/Hf values (Bickford et al., 2010).

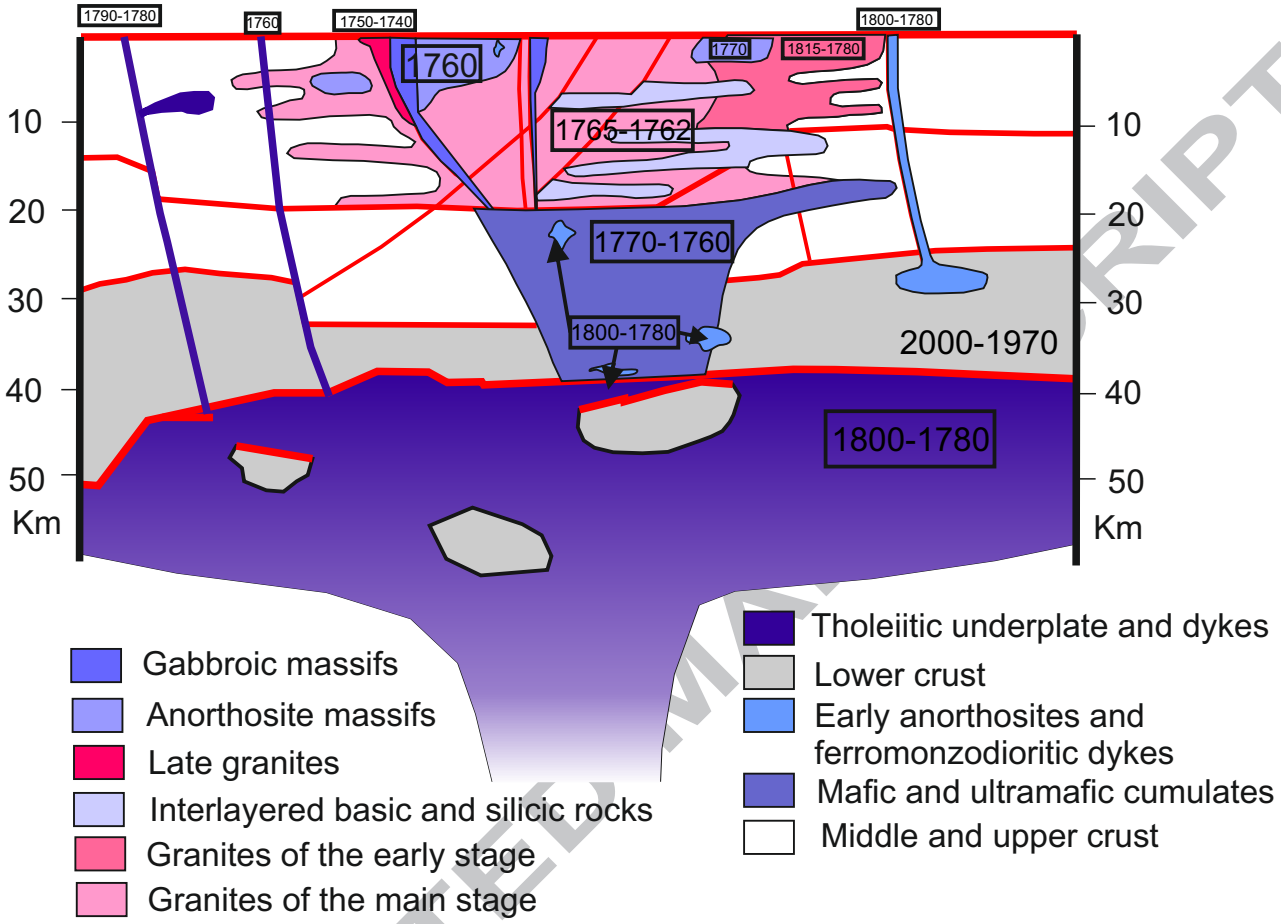

Table 1. Summary of the U-Pb zircon, baddeleyite and allanite ages and Hf isotope ratios of zircons from rocks of the Ukrainian AMCG complexes

	Locality no.	Sample	Age, Ma	Rock	Location	εHf_T	Reference or method
Korosten plutonic complex							
1	1	1/90	1800.0 ± 1.3 (zrn) 1794 ± 7 (bd)	Early anorthosite (A_1)	village Pugachivka	no data	Verkhogliad (1995)
2	2	7/89	1789 ± 2	Early anorthosite (A_1)	Ignatpil quarry	no data	Amelin et al. (1994); Verkhogliad (1995)
3	3	1/89	1784 ± 3	Early anorthosite (A_1)	Granitne quarry (Malyn)	no data	Verkhogliad (1995)
4	3	68	1781 ± 8	Early anorthosite (A_1)	Granitne quarry (Malyn)	0.1 ± 0.4	This study; SIMS
5	4	7/90	1758.1 ± 1.0(zrn) 1760.6 ± 0.7 (bd)	Main anorthosite (A_2)	Holovino quarry	no data	Amelin et al. (1994); Verkhogliad (1995)
6	5	15/90	1758.0 ± 1.8	Main anorthosite (A_2)	Turchynka quarry (Syniy Kamin)	no data	Verkhogliad (1995)
7	5	56/3	1756 ± 4	Main anorthosite, pegmatite (A_2)	Turchynka quarry (Syniy Kamin)	no data	This study; TIMS
8	6	Horbul	1754 ± 4	Main anorthosite, pegmatite (A_2)	Horbuliv quarry	0.0 ± 0.3	This study; TIMS + SIMS
9	7	Parom	1757 ± 3	Main anorthosite, pegmatite	Paromivka quarry	0.0 ± 0.3	This study; TIMS
10	3	10-03	1771.5 ± 0.8 (bd)	Main anorthosite (A_2)	Quarry, Malyn	no data	This study; TIMS
11	8	10/90	1758.8 ± 0.9	Gabbronorite (G_4)	Buky quarry, Buky massif	no data	Amelin et al. (1994); Verkhogliad (1995)
12	9	289/197	1789.8 ± 1.5 (bd)	Gabbro	Davydky massif	no data	This study; TIMS
13	10	599	1761.9 ± 1.6 (zrn + bd)	Olivine gabbro (G_4)	Fedorivka massif, hole 599	-0.8 ± 1.4	This study; TIMS
14	11	03-D24	1763 ± 8	Gabbronorite (G_4)	Pivnichna Slobidka massif, hole	0.4 ± 0.4	This study; SIMS
15	12	03-D18	1756 ± 5	Olivine monzodiorite (G_4)	Torchyn quarry, Torchyn massif	0.1 ± 1.3	This study; SIMS
16	8	71-1M	1761 ± 4	Monzodiorite (G_4)	Buky quarry, Buky massif	no data	This study; SIMS
17	13	23/90	1760.7 ± 1.7	Plagiophyric ferromonzodiorite dyke	village Pugachivka	no data	Amelin et al. (1994); Verkhogliad (1995)
18	14	1025	1799 ± 10	Ferromonzodiorite dyke	Bilokorovychi dyke	no data	Shumlyanskyy and Mazur (2010)
19	15	U8227	1793 ± 3 (bd)	Ferromonzodiorite dyke	Rudnya Bazarska dyke	no data	Shumlyanskyy et al. (2016a)
20	16	06-BG47	1751 ± 12	Ferromonzodiorite sill	Bondary quarry	-3.5 ± 0.5	Lubnina et al. (2009)
21	17	503/105	1810 ± 14	Granite	Northern part of the complex, hole 503	no data	This study; LA-ICP-MS
22	18	75/146	1817 ± 15	Granite	Northern part of the complex, hole 75	no data	This study; LA-ICP-MS
23	16	06-BG48	1780 ± 6	Granite	Bondary quarry	-1.2 ± 1.0	This study; SIMS
24	19	6438	1781 ± 3	Granite porphyry	Usovo village, hole 6438	no data	Amelin et al. (1994)
25	20	53-7	1763 ± 6	Wiborgite	Myrne village	no data	This study; SIMS
26	21	95005	1765 ± 3	Granite	Huta Potiivka village	no data	This study; SIMS
27	22	23/84	1765 ± 5	Granite	City of Malyn, quarry	no data	Scherbak et al. (1989), Amelin et al. (1994), Verkhogliad (1995)

28	23	168-1	1758 ± 5	Subalkaline biotite porphyric granite	Hamarnya village	no data	This study; TIMS
29	24	03-D1	1743 ± 5	Rare-metal granite	Andriivka village	no data	This study; SIMS
30	25	10/87	1752 ± 16	Late granite	Lezniki quarry	no data	Verkhogliad (1995)
31	26	06-E2	1761 ± 13	Rhyolite	Krasylivka village	-1.3 ± 0.3	Shumlyanskyy and Bogdanova (2009)
32	8	71-9	1764 ± 3	Syenite	Buky village	no data	This study; SIMS
33	27	No data	1772 ± 19 1772 ± 6	Syenite	Yastrebetsky massif	no data	Skublov et al. (2014); Sheremet et al. (2012)
Korsun-Novomyrhorod plutonic complex							
34	28	KN-1/2	1756 ± 7 *1801 ± 10*	Early anorthosite (xenolith)	Kamyanka village	no data	Shestopalova et al. (2014), This study; TIMS
35	28	KN-1	1750.2 ± 0.9	Anorthosite	Kamyanka village, Novomyrhorod massif	no data	Dovbush et al. (2009)
36	29	2004	1756 ± 4	Anorthosite	Smila massif, hole 2004	-3.1 ± 0.5	This study; SIMS
37	30	No data	1750.1 ± 1.2	Troctolite	Voronivka village	no data	Shestopalova et al. (2013)
38	31	No data	1749 ± 0.5	Norite	Khlystunivka village	no data	Shestopalova et al. (2013)
39	31	No data	1739 ± 3	Leuconorite	Khlystunivka village	no data	Shestopalova et al. (2013)
40	29	2006	1756 ± 4 (zrn) 1755 ± 6 (zrn + bd)	Olivine-ilmenite norite	Nosachiv massif, hole 2006	-3.0 ± 0.5	This study; SIMS + TIMS
41	29	2008	1757 ± 4 (zrn) *1766.4 ± 1.8 (bd)*	Ilmenite norite	Nosachiv massif, hole 2008	-3.5 ± 0.8	This study; SIMS (zrn) This study; TIMS (bd)
42	32	KN-14-6	1753 ± 7	Olivine-amphibole monzonite dyke	Vyazivok village	no data	Dovbush et al. (2009)
43	31	06-BG4	1746 ± 9	Quartz monzonite	Khlystunivka quarry	-2.8 ± 0.8	This study; SIMS
44	31	06-BG5	1748 ± 7	Quartz syenite	Khlystunivka quarry	-2.9 ± 0.9	This study; SIMS
45	33	KN-15-1	1753.9 ± 0.8 (all)	Wiborgite	Sivach quarry, city of Korsun-Shevchenkivsky	-2.4 ± 0.9	Shestopalova et al. (2010)
46	34	KN-13	1753.7 ± 1.1 (all)	Wiborgite	Shpola massif, Prudyansky quarry	no data	Shestopalova et al. (2010)
47	35	748	1752 ± 12	Granite	Tashlyk village, quarry	no data	Scherbak et al. (2008)
48	34	KH-13	1747 ± 4	Wiborgite	Shpola massif, Prudyansky quarry	no data	Shestopalova et al. (2013)
49	34	KH-13-1	1748 ± 4	Pegmatite in the granite rapakivi	Shpola massif, Prudyansky quarry	no data	Shestopalova et al. (2013)
50		8568/240	1758 ± 3	Granite	Ruska Polyana massif, hole 8568	no data	Ponomarenko et al. (2011)

All data are results of zircon (zrn) dating, if otherwise is not stated; bd – baddeleyite, all - allanite.

Table 2. Results of SIMS U-Pb zircon dating of rocks of the Korosten and Korsun-Novomyrhorod plutonic complexes

	sotope ratios		ages, Ma ± 1σ, %	Concentrations, ppm										
Analysis	$^{207}Pb/^{235}U$	σ, %	$^{206}Pb/^{238}U$	± σ, %		$^{207}Pb/^{206}Pb$	σ, %	disc. %	$^{207}Pb/^{206}Pb$	$^{207}Pb/^{235}U$	$^{206}Pb/^{238}U$		Th	Th/U
Korosten AMCG plutonic complex														
Sample 68, early anorthosite (A_1)														
1	.7710	.4	.3171	.3	1.92	.1091	.6	0.6	785 ± 10	780 ± 12	776 ± 21	82	97	2
2	.7523	.4	.3185	.3	1.90	.1082	.6	.8	770 ± 11	777 ± 12	782 ± 20	53	70	9
3	.5409	.3	.3053	.2	1.86	.1079	.7	3.0	764 ± 12	739 ± 11	718 ± 18	220	143	01
4	.7465	.3	.3159	.2	1.92	.1090	.5	0.8	782 ± 9	776 ± 11	770 ± 18	31	04	00
5	.7771	.4	.3190	.2	1.88	.1086	.7	.5	776 ± 12	781 ± 12	785 ± 20	9	17	6
6	.7660	.5	.3170	.4	1.93	.1090	.6	0.5	784 ± 10	779 ± 13	775 ±21	9	00	4
Sample Horbul, pegmatite in anorthosite of the														

main anorthosite series (A_2), Horbuliv quarry														
1	.2717	.6	.2849	.12	.83	.1088	.5	10.4	779 ± 27	688 ± 44	616 ± 34	8	0	6
2	.0468	.4	.2726	.12	.90	.1077	.0	13.2	753 ± 16	644 ± 39	554 ± 33	04	68	4
3	.1402	.5	.2800	.12	.84	.1072	.4	10.4	760 ± 25	662 ± 42	592 ± 34	1	4	4
4	.5908	.7	.3204	.81	.68	.1039	.0	.5	696 ± 36	748 ± 23	792 ± 29	04	5	5
5	.6515	.1	.3130	.12	.68	.1078	.2	0.5	763 ± 41	759 ± 26	755 ± 32	5	7	7
Sample 03-D24, gabbro (G_4), Pivnichna Slobidka massif														
1	.5092	.1	.3033	.01	.98	.1078	.2	3.6	763 ± 4	733 ± 9	708 ± 16	292	242	42
2	.6267	.1	.3083	.01	.92	.1089	.4	3.1	780 ± 8	754 ± 9	732 ± 15	86	41	6
3	.7225	.2	.3214	.81	.85	.1066	.1	.6	742 ± 21	771 ± 18	797 ± 29	45	39	19
4	.6148	.0	.3098	.81	.92	.1080	.8	1.7	766 ± 15	752 ± 17	740 ± 28	88	89	21
5	.7181	.2	.3175	.91	.86	.1078	.1	.0	762 ± 20	771 ± 18	778 ± 29	32	20	34
6				1										

	.7336	.5	.2473	.0	.66	.1095	.2	22.8	791 ± 21	579 ± 12	424 ± 13	3	5	7
Sample 03-D18, gabbro (G_4), Torchyn massif														
1	.5865	.2	.3065	1.0	.89	.1085	.5	3.3	775 ± 10	747 ± 10	723 ± 16	53	06	2
2	.6482	.1	.3100	1.8	.88	.1088	.0	2.5	779 ± 18	758 ± 18	741 ± 28	66	77	83
3	.7384	.2	.3223	1.9	.86	.1066	.1	.8	743 ± 20	774 ± 19	801 ± 30	55	62	81
4	.1561	.0	.2808	1.0	.99	.1073	.1	10.2	755 ± 3	665 ± 9	596 ± 15	655	240	25
5	.7337	.2	.2518	1.1	.94	.1075	.4	19.7	758 ± 7	579 ± 9	448 ± 14	72	26	27
Sample 71-1M, monzogabbro (G_4), Buky massif, village Buky														
1	.6139	.7	.3107	0.7	.96	.1077	.2	1.1	761 ± 4	752 ± 6	744 ± 10	69	3	02
2	.8136	.7	.3245	0.7	.97	.1076	.2	.4	759 ± 3	787 ± 6	812 ± 11	28	85	15
3	.7317	.8	.3184	0.7	.86	.1078	.4	.3	762 ± 7	773 ± 7	782 ± 11	32	1	2
4	.7722	.0	.3214	0.8	.75	.1077	.7	.3	761 ± 12	780 ± 9	797 ± 12	9	2	1

5	.7638	.9	.3204	0.7	.80	.1078	.5	.9	763 ± 9	779 ± 7	792 ± 11	6	5	5
6	.8006	.8	.3228	0.7	.91	.1079	.3	.6	764 ± 6	785 ± 7	803 ± 11	32	8	1
Sample 06-BG48, granite of the main intrusive phase, Bondary quarry														
1	.3755	.3	.2932	1.3	.98	.1082	.2	7.2	770 ± 4	708 ± 11	658 ± 19	20	67	58
2	.4575	.5	.2980	1.1	.71	.1085	.1	5.9	774 ± 19	723 ± 12	681 ± 16	04	69	82
3	.6702	.3	.3115	1.3	.99	.1088	.1	2.0	779 ± 3	762 ± 11	748 ± 20	96	07	28
4	.9084	.6	.2627	1.6	.97	.1079	.4	16.6	764 ± 7	615 ± 13	504 ± 21	96	98	30
5	.5854	.4	.3058	1.4	.99	.1087	.2	3.7	778 ± 4	747 ± 12	720 ± 21	28	65	02
Sample 53-7, wiborgite of the main intrusive phase, village Myrne														
1	.5681	.0	.3113	0.7	.72	.1064	.7	.6	739 ± 12	744 ± 8	747 ± 11	9	3	5
2				0										

	.6912	.8	.3162	.7	.89	.1076	.4	.8	759 ± 7	766 ± 6	771 ± 11	71	42	3
3	.6365	.8	.3114	0.7	.85	.1080	.4	1.2	766 ± 8	756 ± 7	748 ± 10	67	42	0
4	.6653	.8	.3129	0.7	.86	.1081	.4	0.9	768 ± 8	761 ± 7	755 ± 11	13	3	5
5	.6582	.8	.3143	0.7	.88	.1075	.4	.3	757 ± 7	760 ± 6	762 ± 10	65	41	0
6	.7080	.7	.3158	0.7	.93	.1081	.3	.1	768 ± 5	769 ± 6	769 ± 10	17	46	87
Sample 95005, rapakivi-group granite of the main intrusive phase, village Huta Potievka														
1	.6681	.9	.3124	0.7	.75	.1084	.6	1.3	773 ± 11	762 ± 8	752 ± 11	8	0	3
2	.7541	.7	.3189	0.7	.97	.1081	.2	.1	768 ± 3	777 ± 6	784 ± 11	19	90	91
3	.6877	.0	.3135	0.7	.69	.1084	.7	1.0	774 ± 13	765 ± 8	758 ± 11	3	9	8
4	.6959	.9	.3158	0.7	.72	.1078	.6	.4	763 ± 12	767 ± 8	769 ± 10	2	2	1
5	.8309	.7	.3246	0.7	.99	.1079	.1	.1	765 ± 2	790 ± 6	812 ± 11	608	592	29
6	.7071	.9	.3178	0.7	.79	.1074	.5	.5	756 ± 10	769 ± 7	779 ± 11	6	0	8
7				0										

	.7192	.8	.3182	.7	.83	.1076	.5	.4	759 ± 8	771 ± 7	781 ± 11	11	00	9
Sample 71-9, syenite, village Buky														
1	.1404	.9	.2794	0.8	.96	.1075	.2	10.8	757 ± 4	662 ± 7	588 ± 12	42	89	01
2	.7884	.7	.3222	0.7	.98	.1078	.1	.5	762 ± 3	783 ± 6	801 ± 11	067	59	71
3	.6157	.7	.3102	0.7	.98	.1079	.2	1.5	765 ± 3	752 ± 6	742 ± 11	02	95	74
4	.7597	.7	.3201	0.7	.97	.1078	.2	.8	763 ± 3	778 ± 6	790 ± 11	78	40	97
5	.6411	.7	.3123	0.7	.95	.1078	.2	0.7	762 ± 4	757 ± 6	752 ± 11	89	51	92
6	.6815	.7	.3140	0.7	.97	.1081	.2	0.5	768 ± 3	764 ± 6	760 ± 11	57	22	14
Sample 03-D1, granite vein of the third intrusive phase, Andriivka village														
1	.3850	.1	.2930	1.1	.98	.1085	.2	7.6	775 ± 4	710 ± 10	656 ± 15	595	249	25
2	.5712	.5	.2514	4.1	.92	.1030	.8	15.5	680 ±33	543 ± 36	446 ± 54	34	56	92
3	.1913	.6	.2851	2.6	.99	.1066	.3	8.1	743 ± 6	672 ± 21	617 ± 37	311	045	88
4				1										

	.5494	.3	.3094	.3	.98	.1067	.3	0.4	743 ± 5	740 ± 11	738 ± 20	27	93	60
Korsun-Novomyrhorod AMCG plutonic complex														
Sample 06-BG4, quartz monzonite, Khlystunivka quarry														
1	.4069	.47	.2968	1.37	.93	.1077	.54	5.5	761 ± 10	714 ± 12	675 ± 20	21	33	84
2	.6240	.25	.3141	1.14	.91	.1068	.51	.0	745 ± 9	754 ± 11	761 ± 18	47	4	0
3	.3990	.61	.2995	1.57	.98	.1065	.35	3.4	741 ± 6	712 ± 13	689 ± 23	85	10	1
Sample 06-BG5, quartz syenite, Khlystunivka quarry														
1	.4604	.4	.3029	1.4	.99	.1068	.2	2.6	746 ± 4	724 ± 11	706 ± 20	57	31	40
2	.9204	.5	.2082	2.4	.93	.1017	.0	28.9	656 ± 18	387 ± 19	220 ± 26	46	2	8
3	.4982	.3	.3058	1.3	.98	.1067	.2	1.5	744 ± 5	731 ± 11	720 ± 20	82	03	13
4	.9907	.5	.2719	2.3	.9	.1064	.8	12	739 ±	632 ±	551 ±	54	94	98

					4			.2	15	20	32			
5	.6029	.8	.0598	5 .9	.8 6	.0731	.4	65 .0	017 ± 68	79 ± 26	75 ± 21	66	82	8
Sample 2006, olivine-ilmenite norite, Nosachiv massif														
1	.6404	.9	.3129	1 .6	.8 6	.1076	.0	0. 2	759 ± 18	757 ± 16	755 ± 25	23 1	76	93
2	.6356	.5	.3129	1 .4	.0 0	.1075	.1	0. 1	757 ± 2	756 ± 12	755 ± 22	35 1	00 5	24 5
3	.6069	.3	.3114	1 .3	.9 9	.1073	.2	0. 4	754 ± 4	751 ± 11	748 ± 19	32 9	46 2	27
4	.7262	.5	.3199	1 .3	.8 7	.1072	.7	.5	752 ± 13	772 ± 13	789 ± 20	00	5	1
5	.6646	.5	.3126	1 .2	.8 5	.1082	.8	1. 0	770 ± 14	761 ± 12	754 ± 19	3	8	6
Sample 2008, ilmenite norite, Nosachiv massif														
1	.5822	.4	.3090	1 .4	.9 6	.1075	.4	1. 4	758 ± 7	746 ± 12	736 ± 21	28	32	41
2	.5928	.4	.3111	1 .3	.9 2	.1071	.5	0. 3	750 ± 10	748 ± 12	746 ± 19	49	2	9
3	.6145	.5	.3113	1 .4	.9 5	.1075	.5	0. 7	757 ± 9	752 ± 13	747 ± 22	76	02	22
4	.5896	.3	.3095	1 .3	.9 9	.1076	.2	1. 3	759 ± 4	747 ± 11	738 ± 20	13 6	02 7	94

5	.5256	.3	.3045	.3	1	.98	.1078	.3	3.2	762 ± 5	736 ± 11	714 ± 20	89	46	13
6	.5301	.4	.3064	.4	1	.99	.1072	.2	2.0	753 ± 4	737 ± 12	723 ± 21	264	812	84
Sample 2004, anorthosite of the Smila massif, host to the Nosachiv massif															
1	.4938	.6	.3039	.6	1	.99	.1073	.2	2.8	753 ± 3	730 ± 13	711 ± 24	387	707	03
2	.4466	.5	.3004	.5	1	.99	.1073	.2	4.0	755 ± 3	721 ± 13	693 ± 22	168	218	81
3	.5703	.5	.3080	.5	1	.97	.1076	.4	1.8	759 ± 7	744 ± 13	731 ± 22	70	64	57
4	.5781	.4	.3070	.2	1	.86	.1082	.7	2.8	769 ± 13	745 ± 11	726 ± 18	11	95	9
5	.6247	.2	.3111	.2	1	.96	.1078	.3	1.1	763 ± 6	754 ± 10	746 ± 18	37	90	03
6	.2149	.5	.1449	.5	1	.98	.1109	.3	55.4	814 ± 5	186 ± 11	72 ± 12	36	49	83

Table 3. Results of TIMS U-Pb zircon and baddeleyite dating of rocks of the Korosten and Korsun-Novomyrhorod plutonic complex

	Isotope ratios					Age, Ma		
Fraction, mineral	$^{207}Pb/^{235}U$	± σ, %	$^{206}Pb/^{238}U$	± σ, %	r	$^{206}Pb/^{238}U$	$^{207}Pb/^{235}U$	$^{207}Pb/^{206}Pb$
Korosten plutonic complex								
Sample Parom, Paromivka village, quarry, pegmatite in A_2 anorthosite								
mixed zircon	4.4156	0.1	0.2981	0.1	0.92	1682	1715	1756
mixed zircon	4.5942	0.4	0.3089	0.2	0.66	1735	1748	1764
<0.1 mm zircon	4.2740	1.1	0.2873	1.1	0.99	1628	1688	1764
>0.1 mm zircon	4.0753	1.1	0.2752	1.1	1.0	1567	1649	1756
Sample 56/3, Turchinka village, Syniy Kamin quarry, pegmatite in A_2 anorthosite								
<0.1 mm zircon	4.2665	1.1	0.2874	1.1	1.0	1629	1687	1760
>0.1 mm zircon	4.3794	1.1	0.2958	1.1	1.0	1670	1708	1756
0.1-0.2 mm zircon	4.3591	1.1	0.2944	1.1	1.0	1663	1705	1756
Sample Horbul, Horbuliv village, quarry, pegmatite in A_2 anorthosite								
mixed zircon	4.0403	2.0	0.2779	1.9	1.0	1581	1642	1722
0.1-0.2 mm zircon	4.1475	1.1	0.2794	1.1	1.0	1588	1664	1760
<0.1 mm zircon	4.1716	1.1	0.2815	1.1	1.0	1599	1668	1757
>0.2 mm zircon	4.2530	1.1	0.2873	1.1	1.0	1628	1684	1755
Sample 10-03, city of Malyn, quarry, anorthosite A_2 of the Fedorivka anorthosite massif								
baddeleyite	4.7731	0.1	0.3197	0.1	0.93	1788	1780	1771
baddeleyite	4.7471	0.1	0.3181	0.1	0.91	1780	1776	1770
baddeleyite	4.7542	0.2	0.3182	0.2	0.97	1781	1777	1772
baddeleyite	4.8633	0.9	0.3254	0.9	0.99	1816	1796	1773
baddeleyite	4.7664	0.6	0.3191	0.6	0.99	1785	1779	1772
Sample 599, Fedorivka gabbroic massif, olivine gabbro								
zircon	4.6426	0.3	0.3125	0.3	1.0	1762	1757	1753
zircon	4.6381	0.2	0.3118	0.2	0.9	1764	1756	1750
baddeleyite	4.7066	0.2	0.3167	0.2	0.92	1774	1768	1762
baddeleyite	4.6621	0.8	0.3142	0.8	0.98	1762	1761	1759
baddeleyite	4.6251	0.3	0.3115	0.3	1.0	1761	1754	1748
baddeleyite	4.5770	0.4	0.3082	0.4	1.0	1761	1745	1732
Sample 289/197, Davydky layered gabbro-syenite intrusion, gabbro								
baddeleyite	4.7748	0.2	0.3165	0.2	0.95	1790	1781	1772
baddeleyite	4.7904	0.2	0.3175	0.2	0.95	1790	1783	1777
baddeleyite	4.8017	0.6	0.3190	0.5	0.87	1786	1785	1785
Sample 168-1, Hamarnya village, biotite porphyre granite								
zircon	3.7986	0.2	0.2548	0.1	0.9	1463	1592	1768
zircon	4.0751	0.2	0.2738	0.2	0.9	1560	1649	1765
zircon	4.3223	0.8	0.2910	0.8	1.0	1647	1698	1761
Korsun-Novomyrhorod plutonic complex								
Sample 2006, Nosachiv body, olivine-ilmenite norite								
baddeleyite	4.5547	0.7	0.3066	0.6	0.94	1724	1741	1762
Sample 2008, Nosachiv body, ilmenite norite								
baddeleyite	4.6981	0.2	0.3159	0.1	0.92	1770	1767	1764
baddeleyite	4.7144	0.1	0.3158	0.1	0.84	1769	1770	1771
Sample KN-1/2, xenolith of old anorthosite in anorthosite of the main phase, Kamyanka village								
zircon	4.3080	1.1	0.2938	1.1	1.0	1660	1695	1738
zircon	4.5473	0.1	0.3070	0.1	0.91	1726	1740	1756
zircon	4.7881	0.4	0.3228	0.4	0.99	1804	1783	1759

Table 4. Results of U-Pb LA-ICP-MS dating of zircons from granites of the northern part of the KPC

	sotope ratios			ges, Ma, ± 1σ	Concentrations, ppm										
pot #	$^{06}Pb/^{204}Pb$	$^{06}Pb/^{238}U$	σ, %	$^{07}Pb/^{235}U$	± σ, %	$^{07}Pb/^{206}Pb$	σ, %		isc. %	$^{06}Pb/^{238}U$	$^{07}Pb/^{235}U$	$^{07}Pb/^{206}Pb$		b	h/U
Sample 503/105, granite															
	7480	.3225	.2	.9369	1.5	.1110	.9	.81	1	802 ± 19	809 ± 13	816 ± 16	1	4	.37
	155	.3259	.9	.9507	1.4	.1102	.1	.63		818 ± 14	811 ± 12	802 ± 20	8		.42
	6327	.2983	.0	.4919	1.5	.1092	.2	.62	6	683 ± 15	729 ± 13	787 ± 22	2	1	.58
	0738	.2193	.0	.3843	1.1	.1120	.6	.85	30	278 ± 11	501 ± 9	831 ± 11	2	6	.50
	568	.2966	.6	.6295	1.9	.1132	.0	.86	10	674 ± 24	755 ± 16	851 ± 17	5		.40
	508	.2631	.2	.1553	2.7	.1145	.3	.45	20	506 ± 16	665 ± 22	873 ± 43	9		.57
	9259	.3228	.0	.9198	1.5	.1105	.1	.68		803 ± 16	806 ± 12	808 ± 20	5	3	.46
Sample 75/146, granite															

	12976	.2864	.2	.2639	1.6	.1080	.2	.72	8	623 ± 18	686 ± 14	766 ± 21	87	2	.48
	216	.2624	.6	.1972	2.3	.1160	.6	.68	21	502 ± 21	673 ± 19	895 ± 30	7	3	.33
	158	.3245	.3	.9895	1.5	.1115	.8	.85	1	811 ± 20	818 ± 13	825 ± 14	6	9	.75
	2328	.32400	.9	.9651	1.1	.1112	.7	.82		809 ± 14	813 ± 10	818 ± 11	5	3	.38
	769	.2907	.9	.4213	1.1	.1103	.7	.74	9	645 ± 12	716 ± 10	805 ± 14	8	9	.50
	1520	.2896	.3	.3056	1.5	.1078	.8	.84	7	640 ± 19	694 ± 12	763 ± 10	2	7	.47

Table 5. Hf isotope composition in zircons from rocks of the Korosten and Korsun-Novomyrhorod plutonic complexes

#	$^{178}Hf/^{177}Hf$	±1σ	$^{176}Lu/^{177}Hf$	$^{176}Yb/^{177}Hf$	±1σ	$^{176}Hf/^{177}Hf$ ± 1σ	$^{176}Hf/^{177}Hf_T$	εHf_T	±2σ
Korosten plutonic complex									
Sample 68, early anorthosite (1781.3 ± 7.5 Ma)									
1	1.46727 ± 3	0.00018	0.00644	0.00032		0.281658 ± 11	0.281652	0.1	0.8
2	1.46730 ± 3	0.00008	0.00328	0.00005		0.281672 ± 12	0.281669	0.7	0.8
3	1.46728 ± 2	0.00008	0.00317	0.00004		0.281649 ± 13	0.281647	-0.1	0.9
4	1.46724 ± 2	0.00011	0.00396	0.00005		0.281648 ± 11	0.281644	-0.2	0.8
5	1.46724 ± 3	0.00036	0.01555	0.00032		0.281664 ± 16	0.281651	0.1	1.2
Sample Parom, pegmatite in anorthosite of the main anorthosite series, Paromivka quarry (1758.2 ± 3.7 Ma)									
1	1.46729 ± 3	0.00140	0.05348	0.00069		0.281709 ± 14	0.281662	-0.1	1.0
2	1.46727 ± 3	0.00212	0.08528	0.00088		0.281715 ± 19	0.281644	-0.7	1.4
3	1.46728 ± 2	0.00164	0.06117	0.00010		0.281726 ± 14	0.281671	0.3	1.0
4	1.46730 ± 3	0.00089	0.02894	0.00054		0.281716 ± 16	0.281686	0.8	1.1
Sample Horbul, pegmatite in anorthosite of the main anorthosite series, Horbuliv quarry (1758.2 ± 3.7 Ma)									
1	1.46726 ± 4	0.00051	0.02143	0.00094		0.281690 ± 18	0.281672	0.3	1.3
2	1.46725 ± 3	0.00043	0.01680	0.00044		0.281675 ± 14	0.281661	-0.1	1.0
3	1.46728 ± 3	0.00059	0.02123	0.00037		0.281683 ± 11	0.281663	0.0	0.8
4	1.46725 ± 3	0.00066	0.02605	0.00008		0.281687 ± 14	0.281665	0.0	1.0
5	1.46728 ± 3	0.00065	0.02684	0.00014		0.281653 ± 17	0.281631	-1.2	1.2
Sample 599, olivine gabbro, Fedorivka massif (1762.3 ± 1.6 Ma)									
1	1.46726 ± 3	0.00052	0.01548	0.00034		0.281657 ± 11	0.281639	-0.8	0.8
2	1.46719 ± 3	0.00097	0.03108	0.00039		0.281686 ± 13	0.281653	-0.3	1.0
3	1.46726 ± 3	0.00074	0.02173	0.00149		0.281640 ± 18	0.281615	-1.6	1.3
Sample 03-D24, gabbro, Pivnichna Slobidka massif (1763.1 ± 8.4 Ma)									
1	1.46725 ± 3	0.00098	0.03655	0.00019		0.281715 ± 16	0.281682	0.8	1.2
2	1.46724 ± 2	0.00054	0.02018	0.00035		0.281680 ± 12	0.281662	0.1	0.9
3	1.46725 ± 2	0.00065	0.02464	0.00027		0.281705 ± 11	0.281684	0.8	0.8
4	1.46727 ± 2	0.00095	0.03521	0.00046		0.281686 ± 14	0.281654	-0.2	1.0
5	1.46726 ± 2	0.00073	0.02757	0.00044		0.281697 ± 12	0.281673	0.4	0.9
Sample 03-D18, olivine monzogabbro, Torchyn massif (1756.3 ± 4.6 Ma)									
1	1.46724 ± 2	0.00187	0.07535	0.00086		0.281710 ± 17	0.281648	-0.6	1.2
2	1.46728 ± 2	0.00131	0.05171	0.00121		0.281674 ± 18	0.281630	-1.2	1.3
3	1.46727 ± 2	0.00006	0.00226	0.00002		0.281673 ± 13	0.281671	0.2	0.9
4	1.46725 ± 2	0.00008	0.00332	0.00012		0.281702 ± 12	0.281699	1.2	0.8
5	1.46728 ± 5	0.00067	0.02651	0.00006		0.281662 ± 21	0.281640	-0.9	1.5
Sample 06-BG48, granite of the main intrusive phase, Bondary quarry (1780.4 ± 6 Ma)									
1	1.46726 ± 2	0.00286	0.12297	0.00684		0.281745 ± 17	0.281648	0.0	1.3
2	1.46726 ± 4	0.00182	0.08635	0.00507		0.281666 ± 12	0.281605	-1.6	0.8
3	1.46726 ± 3	0.00260	0.10276	0.01116		0.281678 ± 13	0.281590	-2.1	1.3
4	1.46726 ± 2	0.00228	0.09941	0.01083		0.281713 ± 15	0.281636	-0.5	1.2
5	1.46721 ± 3	0.00234	0.10701	0.00361		0.281685 ± 22	0.281606	-1.5	1.6
Sample 06-BG47, jotunitic dolerite sill, Bondary quarry (1750 ± 12 Ma)									
1	1.46725 ± 2	0.00083	0.03690	0.00028		0.281590 ± 14	0.281563	-3.8	1.0
2	1.46728± 3	0.00197	0.09262	0.00879		0.281640 ± 21	0.281575	-3.3	1.5
3	1.46724 ± 2	0.00047	0.01846	0.00011		0.281600 ± 12	0.281585	-3.0	0.9
4	1.46722 ± 2	0.00154	0.07032	0.00769		0.281592 ± 21	0.281541	-4.5	1.5
5	1.46724 ± 3	0.00102	0.04031	0.00022		0.281608 ± 15	0.281574	-3.4	1.1
Sample 06-HB7, rhyolite, Ovruch basin (1761 ± 13 Ma)									
1	1.46724 ± 1	0.00096	0.03373	0.00108		0.281673 ± 29	0.281641	-0.7	2.1
2	1.46726 ± 2	0.00042	0.01375	0.00021		0.281649 ± 13	0.281635	-1.0	0.9

3	1.46725 ± 2	0.00050	0.01672	0.00029	0.281631 ± 15	0.281615	-1.7	1.1
4	1.46722 ± 3	0.00051	0.01669	0.00085	0.281647 ± 10	0.281630	-1.1	0.7
5	1.46723 ± 3	0.00047	0.01679	0.00014	0.281640 ± 19	0.281625	-1.3	1.4
5	1.46726 ± 5	0.00049	0.01746	0.00026	0.281636 ± 6	0.281620	-1.5	0.4
6	1.46717 ± 2	0.00034	0.01197	0.00031	0.281649 ± 52	0.281638	-0.9	3.7
7	1.46716 ± 3	0.00066	0.02284	0.00214	0.281671 ± 20	0.281649	-0.5	1.4
			Korsun-Novomyrhorod plutonic complex					
Sample 06-BG4, quartz monzonite, Khlystunivka quarry (1746.1 ± 9.1 Ma)								
1	1.46723 ± 2	0.00175	0.07069	0.00187	0.281663 ± 6	0.281605	-2.4	0.4
2	1.46722 ± 2	0.00079	0.03015	0.00151	0.281595 ± 11	0.281569	-3.6	0.8
3	1.46723 ± 2	0.00072	0.02743	0.00067	0.281594 ± 13	0.281570	-3.6	0.9
4	1.46729 ± 2	0.00049	0.01971	0.00040	0.281597 ± 12	0.281581	-3.2	0.8
5	1.46722 ± 3	0.00070	0.02910	0.00102	0.281626 ± 16	0.281603	-2.4	1.1
Sample 06-BG5, quartz syenite, Khlystunivka quarry (1748.0 ± 6.9 Ma)								
1	1.46724 ± 2	0.00236	0.10509	0.00783	0.281639 ± 12	0.281561	-3.9	1.0
2	1.46721 ± 2	0.00166	0.07852	0.01204	0.281620 ± 11	0.281565	-3.7	1.0
3	1.46726 ± 3	0.00121	0.05024	0.00091	0.281652 ± 13	0.281612	-2.1	0.9
4	1.46724 ± 2	0.00101	0.04155	0.00292	0.281627 ± 11	0.281593	-2.7	0.8
5	1.46723 ± 2	0.00046	0.01719	0.00043	0.281615 ± 10	0.281600	-2.5	0.7
Sample 2006, olivine-ilmenite norite, Nosachiv massif (1756.2 ± 3.7 Ma)								
1	1.46717 ± 5	0.00158	0.06421	0.00034	0.281611 ± 35	0.281558	-3.8	2.5
2	1.46723 ± 3	0.00028	0.01060	0.00004	0.281592 ± 12	0.281583	-2.9	0.9
3	1.46723 ± 3	0.00125	0.04990	0.00031	0.281632 ± 19	0.281591	-2.6	1.4
4	1.46726 ± 2	0.00197	0.08352	0.00190	0.281636 ± 16	0.281570	-3.4	1.2
5	1.46724 ± 3	0.00094	0.04997	0.00086	0.281620 ± 17	0.281588	-2.7	1.2
Sample 2008, ilmenite norite, Nosachiv massif (1757.0 ± 4.1 Ma)								
1	1.46727 ± 2	0.00063	0.02448	0.00062	0.281585 ± 13	0.281564	-3.6	0.9
2	1.46725 ± 3	0.00028	0.01041	0.00018	0.281571 ± 13	0.281561	-3.7	0.9
3	1.46723 ± 3	0.00023	0.00989	0.00017	0.281603 ± 16	0.281595	-2.5	1.1
4	1.46725 ± 2	0.00104	0.03952	0.00083	0.281572 ± 16	0.281538	-4.5	1.1
5	1.46723 ± 3	0.00110	0.04213	0.00081	0.281606 ± 16	0.281570	-3.4	1.2
Sample 2004, anorthosite, host to the Nosachiv massif (1754.3 ± 3.9 Ma)								
1	1.46728 ± 2	0.00046	0.01916	0.00041	0.281596 ± 12	0.281580	-3.1	0.9
2	1.46727 ± 3	0.00114	0.04588	0.00012	0.281620 ± 16	0.281582	-3.0	1.1
3	1.46724 ± 3	0.00365	0.15039	0.00188	0.281716 ± 29	0.281594	-2.6	2.0
4	1.46723 ± 3	0.00180	0.07140	0.00068	0.281609 ± 19	0.281549	-4.2	1.4
5	1.46726 ± 2	0.00110	0.04764	0.00018	0.281629 ± 14	0.281593	-2.6	1.0
Sample 06-BG1, wiborgite, Korsun-Shevchenkivsky quarry (1753.9 ± 0.8 Ma)								
1	1.46723 ± 3	0.00111	0.04696	0.00144	0.281640 ± 16	0.281603	-2.2	1.2
2	1.46725 ± 2	0.00154	0.07411	0.00415	0.281680 ± 14	0.281628	-1.4	1.0
3	1.46724 ± 2	0.00050	0.02060	0.00064	0.281624 ± 13	0.281608	-2.1	1.0
4	1.46722 ± 2	0.00185	0.07736	0.00581	0.281644 ± 10	0.281582	-3.0	0.8
5	1.46722 ± 2	0.00066	0.02960	0.00066	0.281603 ± 13	0.281581	-3.0	1.0

Highlights

- Results of 22 new zircon and baddeleyite U-Pb ages obtained for rocks of the Ukrainian AMCG complexes are reported
- 16 zircon samples were analyzed for Hf isotopes
- The long duration of the AMCG magmatism is discussed
- A mixed lower-crustal - mantle source of the parental melts is proposed
- A model of the Ukrainian AMCG complexes formation is offered